# Are populations like a circuit? Comparing isolation by resistance to a new coalescent-based method.

Erik Lundgren,* and Peter L. Ralph†

April 22, 2019

## Abstract

A number of methods commonly used in landscape genetics use an analogy to electrical resistance on a network to describe and fit barriers to movement across the landscape using genetic distance data. These are motivated by a mathematical equivalence between electrical resistance between two nodes of a network and the "commute time", which is the mean time for a random walk on that network to leave one node, visit the other, and return. However, genetic data are more accurately modeled by a different quantity, the coalescence time. Here, we describe the differences between resistance distance and coalescence time, and explore the consequences for inference. We implement a Bayesian method to infer effective movement rates and population sizes under both these models, and find that inference using commute times can produce misleading results in the presence of biased gene flow. We then use forwards-time simulation with continuous geography to demonstrate that coalescence-based inference remains more accurate than resistance-based methods on realistic data, but difficulties highlight the need for methods that explicitly model continuous, heterogeneous geography.

# Introduction

Genetic relatedness is determined by past gene flow, a product of individual or gamete movements across geographic space. Genomes therefore retain the traces of this movement, and can contribute to the inference of how a species moves across a landscape, which is important for understanding how diseases spread, how species adapt, and how to retain genetic diversity in threatened species. This is a potentially important source of information, as direct observation can be difficult (especially of long-distance movement, [Cayuela et al., 2018, Levin et al., 2003]), or even impossible, if some of the populations in question no longer exist.

The idea of "resistance distance" is an important tool in the landscape genomics toolbox. Introduced by McRae [2006], it makes use of a mathematical equivalence between random walks and electrical resistance [Nash-Williams, 1959]: the expected time for a continuous-time Markov chain that starts at node $x$ to first hit node $y$ and then return to $x$ (the "commute time") is equal to the effective resistance between $x$ and $y$ in an electrical network whose conductances are given by the movement rates of the Markov chain [Levin et al., 2008, Doyle and Snell, 2006]. This measure therefore averages over all possible paths through the network between the two. Suppose we assign local conductances based on the values of some landscape variable, and compute the correlation of genetic distances between samples from different parts of the landscape with the effective resistances between the samples' locations. If this results in a significant positive correlation, then this is taken as good evidence that the landscape variable is a good indicator of where gene flow occurs [McRae and Beier, 2007, Cushman et al., 2006]. For instance, if the conductance across a grid cell in a discretization of the landscape is higher in flatter areas, and this produces effective resistance values that are significantly correlated with genetic distances, then one might conclude that the species in question tends to disperse more readily through flatter areas, perhaps along river valleys. More recent methods [Petkova et al.,

---

*Computational Biology, University of Southern California
†Institute for Ecology and Evolution, University of Oregon

1

2016, Hanks and Hooten, 2013] seek to build *de novo* a map of conductance values that produces resistances most strongly correlated with observed genetic distance, and then interpret regions of low conductance in the resulting map as barriers to gene flow.

As motivated by McRae [2006], commute time (i.e., resistance distance) is a computationally tractable approximation to the more accurate random walk-based model of genetic distance, the *coalescence time*. Genetic distances between two genomes sampled from the landscape do derive from an average across a large number of paths between those points – the lineages along which each segment of genetic material has been inherited from their most recent common ancestor. Thanks to recombination, there are a large number of such paths, and genetic distance averages over these. The more recent these common ancestors tend to be, the smaller the genetic distance is. It is reasonable in some situations to model these lineages as random walks across the landscape; however, the model of genetic distance that one is thus led to is *coalescence time* of the random walks, rather than commute time, the quantity that corresponds to resistance. This naturally raises the question: Are methods that depend on effective resistances being misled by model misspecification? If so, would using coalescence time do better?

McRae [2006] showed that coalescence time and resistance distance are equal (up to shift and scaling) in isotropic landscapes such as a ring [Matsen and Wakeley, 2006], and found that the two were highly correlated in several test cases. However, all test cases had symmetric migration (the same rate of gene flow in both directions along each edge), which is likely not the case in many situations, e.g., in rivers [Morrissey and de Kerckhove, 2009, Sundqvist et al., 2016, Hanks, 2017], with source-sink dynamics [Dias, 1996], or after population expansions [With, 2002].

In this paper, we contrast coalescence time and resistance distance, and develop a method to infer movement rates on a discrete landscape using genetic distances. As we will see, although the two methods are conceptually similar, resistance-based inference may infer movement rates uncorrelated with the truth if data are derived from a coalescent process, especially in the presence of gene flow asymmetry. We also explore the question of identifiability. Resistance-based methods are often used to predict distances based on a few layers of geographical data (land cover, slope, etcetera). Some methods find the combination of landscape layers to best explain genetic distance, which allows very fine geographic resolution [Shaffer et al., 2017]. Other methods such as EEMS ["Estimating Effective Migration Surfaces", Petkova et al., 2016] infer conductances without such prior information; however, the geographical resolution is much coarser. (A recently-released method that is based on EEMS but uses haplotype length data and an underlying model of coalescence time [Al-Asadi et al., 2018] is promising, but still produces similarly coarse maps.) One reason for this difference in resolution is that EEMS uses more computationally intensive Bayesian methods. However, we show that this coarse resolution reflects a more general problem, both because of unmodeled "process noise" involved in discretization of geographical populations, and the mathematical structure of the underlying problem.

# Methods

The *commute time* of a Markov chain between locations $i$ and $j$ is the expected time for a particle that moves according to the rules of the chain, started at $i$, to first reach $j$ and then return. We will denote this by $R_{ij}$, to emphasize that it is also the effective resistance between $i$ and $j$. The *coalescence time* is the expected time for two particles started at $i$ and $j$ to *coalesce*, which happens at a given rate whenever they are in the same location. We will denote this by $C_{ij}$. Why should these be related to genetic distance? We first explain this connection and discuss computation of both quantities, and finally develop a method that infers movement rates of the Markov chain (which are rates of gene flow) from observations of coalescence time. We apply the method to both realistic simulations in continuous space and to an empirical dataset. Although we have tried to highlight the intuitive aspects of the initial technical discussion, readers who are interested in practical differences more than the mathematical arguments should be able to skip to "Test cases and simulations" without loss of continuity.

## Genetic distance and coalescence time

There are a number of ways to calculate measures of dissimilarity using genetic data. In this paper we use mean pairwise divergence, which for two genomes is calculated as the proportion of sites in the genome at which the two genomes differ. It is more common in the literature to use $F_{ST}/(1-F_{ST})$, but the two are highly correlated for good theoretical reasons [Slatkin, 1991, Rousset, 1997], especially for SNP data. (However, note that $F_{ST}$ depends on the sampling scheme, while divergence does not.) The two genomes differ at a site only if there has been a mutation in some ancestor on the lineages leading from the two genomes back to their most recent common ancestor at that site. Therefore, under an infinite-sites model with average mutation rate $\mu$ per site and per meiosis, pairwise divergence divided by $\mu$ is an unbiased estimate of the mean time to most recent common ancestor, averaged across the genome [Hudson, 2007, Ralph, 2015]. It is natural to model this process by following the two lineages back through time (and across space) until they find their most recent common ancestor, i.e., until they coalesce. Suppose we model the geographic distribution of the species as a collection of randomly mating populations that exchange occasional migrants, thus discretizing geographic space. It is common to assume that the motion of these lineages back through time forms a Markov process, the *structured coalescent* [Wakeley, 2005]. (This assumption requires the effects of natural selection on each segment of the genome to be generally weak.) In this framework, each lineage performs a random walk across the populations, with movement probabilities depending on the flux of individuals between populations. This provides the link between genetic distance and random walks.

For data, we are given genotypes of individuals and their geographic coordinates; then, we divide these individuals into groups, and compute the genetic distance between group $i$ and group $j$ as the mean divergence between a pair of genomes, chosen one from each group. We denote the resulting genetic distance $D_{ij}$; since divergence is symmetric, $D_{ij} = D_{ji}$. We compute $D_{ii}$ by sampling without replacement from group $i$, so that generally $D_{ii} > 0$: the diagonal elements measure local diversity. As discussed below, "resistance distance" methods find commute times so that the mean commute time between $i$ and $j$ matches $D_{ij}$ – but the commute time of a location to itself is zero, so a term is added to account for local diversity. We do this in the same way as Petkova et al. [2016], by introducing the *local diversity* parameters $q_i$, and using the model

$$D_{ij} \approx \widetilde{R}_{ij} = R_{ij}/4 + q_i/2 + q_j/2. \tag{1}$$

Concretely, this means finding movement rates of a Markov chain whose matrix of commute times ($R$) yields a good approximation to the matrix of genetic distances, after adding local diversity parameters ($q$, which are also free parameters). The factor of four is necessary to make commute time work on the same time scale as coalescence time: the commute time covers the path from $i$ to $j$ twice (once in both directions), while the coalescence time covers the distance only once, and in half the time, because two particles are moving. For a conceptual picture of the differences between the coalescence time and commute time, see Figure 1.

A simple situation when the two clearly differ is in the presence of biased gene flow, as for instance between a source and a sink population: coalescence only requires that lineages move in *one* direction between populations, while a commute requires movement in both.

## Hitting times of Markov chains

Now, we explain how to compute the relevant quantities – mean commute and coalescence times – from a Markov chain model of lineage movement. The Markov chain is defined by its *generator matrix*, denoted $G$, for which $G_{xy}$ gives the "jump rate" from $x$ to $y$. The jump rate $G_{xy}$ is the probability the chain jumps to position $y$ when at position $x$ per unit of time. (More precisely, if the Markov chain is at location $X_t$ at time $t$, then for $x \neq y$, $\mathbb{P}\{X_{t+\epsilon} = y \mid X_t = x\} = \epsilon G_{xy} + O(\epsilon^2)$.) For mathematical convenience, the diagonal of this matrix is completed so that rows sum to zero: $G_{xx} = -\sum_{y \neq x} G_{xy}$. We will need to find the *hitting times* of the chain – i.e., for each pair of states $x$ and $y$, the mean time until the chain first hits $y$ after being started at $x$. We denote this quantity $H_{xy}$. Throughout, we assume that all hitting times are finite, which implies the chain is connected and irreducible. The Markov property lets us write a system of linear equations that can be solved for $H$, as follows (see, e.g., Kemeny and Snell [1983]): Suppose that the chain
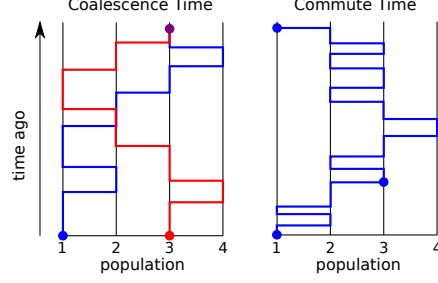
3

Figure 1: Illustration of the conceptual differences between coalescence and commute time between states 1 and 3 for a continuous time Markov chain with four linearly connected states. Coalescence time (left) is the time for two independently moving particles to meet and coalesce (it is possible for them to be in the same location without coalescing). Commute time is time for a single particle starting in one state to travel to another state and then back to the original state. Note how the time axis is scaled to be faster in the figure showing commute time than the one for coalescence time in order for them to fit in the same space.

begins at $x \neq z$, and is at location $y \neq z$ after $dt$ units of time, without having visited $z$. Then the total time to hit $z$ is equal to the elapsed time $dt$ plus the remaining time to hit $z$ from $y$. Taking the average over possible paths, this says that $H_{xz} \approx dt + \sum_y \mathbb{P}\{X_{dt} = y \mid X_0 = x\}H_{yz}$. Replacing $\mathbb{P}\{X_{dt} = y \mid X_0 = x\}$ with $dtG_{xy}$ and rearranging gives the system of equations:

$$\sum_y G_{xy}H_{yz} = -1 \qquad \text{for } x \neq z. \tag{2}$$

In other words, if $G_{-z}$ is the matrix with the $z^{\text{th}}$ row and column removed, and $\mathbf{1}$ is the vector composed of all ones, then the $z^{\text{th}}$ column of $H$, except for $H_{zz}$, can be computed as $-(G_{-z})^{-1}\mathbf{1}$. This, along with $H_{zz} = 0$, allows computation of $H$ from the movement rates $G$ [Kemeny and Snell, 1983].

Suppose instead we are given the hitting times, $H$, and wish to find the movement rates, $G$. This is not the situation we are in – we have either commute or coalescence times – but it is related. The Random Target Lemma [Aldous and Fill, 2002] tells us that the stationary distribution of the Markov chain, denoted $\pi$, can be recovered from the hitting times by solving $\pi = H^{-1}\mathbf{1}/\mathbf{1}^T H^{-1}\mathbf{1}$. As shown in Appendix B, equation (2) can be rewritten in matrix form as

$$GH = \text{diag}(1/\pi) - \mathbf{1}\mathbf{1}^T, \tag{3}$$

which implies that $G$ can be computed directly from $H$ as

$$G = \left(\text{diag}(1/\pi) - \mathbf{1}\mathbf{1}^T\right) H^{-1}. \tag{4}$$

(We prove that $H$ is invertible in Appendix B.) Therefore, the pairwise mean hitting times, $H$, uniquely determine the jump rates, $G$.

The *commute time* between $x$ and $y$ is the mean time a chain started at $x$ takes to first hit $y$ and then to return to $x$. We will write this as

$$\textbf{(commute time)} \qquad R_{xy} = H_{xy} + H_{yx}, \tag{5}$$

or in matrix notation, $R = H + H^T$. Note that the commute times are symmetric, even though the hitting times may not be.

Although commute times are uniquely determined by movement rates, the reverse is not true – we can use equations (3) and (5) to see how to modify movement rates without changing commute times. A small concrete example of this is given in Appendix A. More generally, commute times only depend on the symmetric part of $H$ – given a skew-symmetric matrix $Z$ (so that $Z + Z^T = 0$), any Markov chain that has

4

hitting times given by $H_\epsilon = H + \epsilon Z$ for some number $\epsilon$ will have the same commute times. The resulting hitting times may not be valid – if $G_\epsilon$ is the matrix constructed by applying equation (4) to $H_\epsilon$, then it is not guaranteed that the offdiagonal elements of $G_\epsilon$ are all nonnegative, as required. However, since $G$ and $H$ are continuous functions of each other, if all offdiagonal elements of $G$ are strictly positive, then there exists a positive $\epsilon_0$ such that all $G_\epsilon$ for $\epsilon < \epsilon_0$ do define valid Markov chains, all with the same commute times.

The *coalescence times* are defined using *two* copies of the same chain, as the mean time until coalescence, if the chains coalesce at rate $\gamma$ when they are in the same place. Concretely, suppose that $X$ and $Y$ are independent Markov chains both moving with movement rates given by $G$, that coalesce at rate $\gamma_x$ when $X$ and $Y$ are both at $x$. Define $\tau$ to be this coalescence time, so that $\mathbb{P}\{\tau \leq t + \epsilon \,|\, \tau > t,\, X_t = Y_t = x\} = \epsilon\gamma_x + O(\epsilon^2)$, and $\mathbb{P}\{\tau \leq t + \epsilon \,|\, \tau > t,\, X_t \neq Y_t\} = O(\epsilon^2)$. Then, the (mean) coalescence time is defined to be $C_{xy} = \mathbb{E}[\tau \,|\, X_0 = x, Y_0 = y]$. An argument similar to the one behind equation (2) shows that the coalescence times satisfy the following system of equations:

$$\textbf{(coalescence time)} \qquad \sum_y (G_{xy}C_{yz} + C_{xy}G_{zy}) = \begin{cases} -1 & \text{if } x \neq z, \\ -1 + \gamma_z C_{zz} & \text{if } x = z. \end{cases} \qquad (6)$$

Similar recursions are common in the literature, going back at least to Hill [1972] (see also Whitlock and Barton [1997]). In matrix notation, this is

$$GC + CG^T - \text{diag}(\gamma) \circ C = -\mathbf{1}\mathbf{1}^T, \qquad (7)$$

where $\text{diag}(\gamma)$ is the matrix with the vector $\gamma$ on the diagonal and zeros elsewhere, and $\circ$ is the componentwise product. In practice, we solve this by working with the product Markov chain $(X_t, Y_t)$, whose generator matrix is $G \otimes I + I \otimes G$, where $I$ is the identity matrix and $\otimes$ is the Kronecker product.

Equation (7) is linear in $G$ and $\gamma$, and so after rearrangement can be solved with standard linear algebra (and is related to the Sylvester equation [Bhatia and Rosenthal, 1997]). However, the solution is again not necessarily unique: suppose that we have a matrix $Z$ such that $ZC$ is skew-symmetric. Then $(G + Z)C + C(G + Z)^T = GC + CG^T$, and so a Markov chain with generator matrix $G + Z$ has the same coalescence times as the original chain. Furthermore, for $G + Z$ to be a valid generator of a Markov chain, the rows of $Z$ must sum to zero, and all offdiagonal entries of $G + Z$ must be nonnegative. As before, if all entries of $G$ are nonzero, it is always possible to find sufficiently small $\epsilon$ so that $G + \epsilon Z$ remains the generator of a valid Markov chain. The coalescence rates, $\gamma$, provide additional degrees of freedom which may render solutions nonunique in a broader range of situations.

**Constraints and uniqueness** We have seen that to find the movement rates of a continuous-time Markov chain given the coalescence or commute times we must solve either equation (7) or equations (4) and (5) for $G$, and that these do not have unique solutions. The situation is worse when one needs to infer coalescence rates ($\gamma$) as well. However, usually in applications the locations lie across geographical space, so that many of the entries of $G$ can be assumed to be zero. This reduces the number of unknowns to solve for, and so can render the solution unique. We can get an idea of this by simply counting equations and unknowns. For concreteness, suppose that the spatial locations are arranged in a square grid of $n$ locations, so that each is connected to four others. (Boundary locations will have fewer, but we omit this detail.) Since movement rates in each direction can be different, there are $4n$ free parameters, each corresponding to an off-diagonal entry of $G$. Coalescence rates provide another $n$ parameters.

Since coalescence times are symmetric, equation (7) provides $n(n + 1)/2$ informative equations. This is larger than $4n + n$, the number of parameters, for a grid with at least nine nodes (i.e., $3 \times 3$), so we would expect the system of equations to usually have a unique solution for grids larger than this, although some special cases will still have free parameters. The same calculation holds for commute times except that there are $n$ local diversity parameters instead of $n$ coalescence parameters.

This suggests that nonuniqueness of solutions may not be a problem in practice, as long as geography is discretized into sufficiently many regions and direct, long-distance migration is disallowed (i.e., parents and offspring live in the same or neighboring regions). However, finer geographic resolutions may present problems

5

of nonidentifiability, similar to the problem of multiple linear regression with many collinear variables. The problem of inferring gene flow rates on fine geographic maps may become *ill-conditioned*, i.e., arbitrarily small variations in the data (even numerical instability) may produce large differences in the inferred "best" rates. Information about the landscape contained in higher-order modes (e.g., finer resolution changes in hitting times) is obscured by noise. (For the interested technical reader, this could occur as the spatial resolution increases because the matrix $G$ converges to a second-order elliptic differential operator [Stroock and Varadhan, 1997]; such operators are deformations of the Laplacian [Feller, 1957], which has rapidly decaying eigenvalues [McKean and Singer, 1967, Kuttler and Sigillito, 1984].) This implies a fundamental limit to the geographical resolution of inferred maps. For more discussion of related problems, see Epstein and Schotland [2008], Myers et al. [2008], or Terhorst and Song [2015].

One strategy for circumventing ill-conditioning is to impose additional constraints – for instance, constraining all population sizes to be the same (something we do below), or allowing only two distinct migration rates: one rate across a barrier, and another across "non-barriers". Such constraints amount to a form of regularization, since they look for solutions to the original problem with certain desirable properties (e.g., most of the values are the same).

**When are coalescence and commute times equal?** If in a given biological situation commute and coalescence times are equal – i.e., if given $G$ and $\gamma$, there was a $q$ that made $C = \widetilde{R}$ – then inference with either model would be equivalent. This was demonstrated in some situations by McRae [2006]. We have already shown that this is not the case in general, but it turns out that it *is* true under some restrictive assumptions commonly found in abstract population genetics models. We show in Appendix C that if hitting times are symmetric ($H = H^T$), then this does occur, and so the two methods are equivalent for symmetric island models (where the populations are arranged on a ring and migration rates only depend on the distance between them). Hitting times are not symmetric for a square grid with uniform migration (the mean time to hit the center from a corner is less than the reverse), but the square grid is quite close to the torus, which does have symmetric hitting times.

# Bayesian inference of movement rates

Mean coalescence times estimated from real data are subject to a number of sources of noise (which we discuss in more detail later). Here, we use exact solutions of the equations above to develop a Bayesian inference method that accounts for noise in the data and estimates uncertainty in the resulting estimates. To do this, we model genetic distances as equal to coalescence times plus noise: $D_{ij} = C_{ij} + \epsilon_{ij}$, where $\epsilon_{ij}$ are independent and Gaussian distributed with mean $\mathbf{0}$ and variance $\sigma_\epsilon^2$, except that $\epsilon_{ij} = \epsilon_{ji}$. (We assume that coalescence times are measured to good accuracy – i.e., $C_{ij}$ is large compared to $\sigma_\epsilon$ – so that this model does not predict negative times.) Given $G$ and $\gamma$ we can solve equation (7) to find the corresponding coalescence times – which we call $\mathcal{C}(G, \gamma)$ – so our model is that $D$ has a Gaussian distribution with mean $\mathcal{C}(G, \gamma)$. (This Gaussian stands in for the sampling noise of coalescence times about their mean.) The maximum likelihood estimate of $G$ could be found directly; however, this in practice will quite likely contain negative movement rates, and does not allow us to impose constraints (such as only allowing a subset of movement rates to be nonzero).

Therefore, we use Bayesian inference, placing independent exponential priors on the parameters – the movement rates, $G_{ij}$, that are not constrained to be zero and the coalescence rates, $\gamma$. Concretely, suppose that the spatial arrangement of populations is given by a graph (i.e., a discrete collection of locations represented by "nodes", between which movement is possible only between those connected by "edges"). Only movement rates in $G$ that correspond to edges in the graph are allowed to be nonzero. Suppose there are $m_G$ edges in the graph, that each of the $n$ populations has its own coalescence rate, and write $i \sim j$ to

mean that $i$ and $j$ are adjacent in the graph. Then, the resulting log-posterior density is

$$\mathcal{L}(D, G, \gamma) = 2m_G \log(\lambda_G) + n \log(\lambda_\gamma) - \frac{n(n+1)}{2} \log(2\pi\sigma_\epsilon^2) - \sum_{i \sim j} \lambda_G G_{ij}$$

$$- \sum_{i=1}^{n} \lambda_\gamma \gamma_i - \frac{1}{2\sigma_\epsilon^2} \sum_{i \leq j} (\mathcal{C}_{ij}(G, \gamma) - D_{ij})^2 \tag{8}$$

Here $1/\lambda_\gamma$ and $1/\lambda_G$ are the prior means of $\gamma_i$ and $G_{ij}$, respectively. Recall that both $D$ and $\mathcal{C}(G, \gamma)$ are full matrices of pairwise distances between discrete locations (in the same order), and so the term $(\mathcal{C}_{ij}(G, \gamma) - D_{ij})^2$ measures the deviation of the observed genetic distances from those predicted under the coalescent model on the graph.

Inference with resistance distance is done in exactly the same way, except that $q$ replaces $\gamma$, and instead of $\mathcal{C}(G, \gamma)$ we use $\widetilde{\mathcal{R}}(G, q)$, which is the matrix $\widetilde{R}$ computed from $G$ and $q$ by putting the solution to equation (2) through equations (5) and (1).

It is not required in this approach to have samples from every spatial location, allowing inference on incompletely sampled spatial discretizations. (However, more complete sampling will produce more accurate results.) To carry out inference in this situation, we simply use Equation 8, but only sum over observed entries of $D_{ij}$.

**MCMC methods**   To sample from the posterior distribution of equation (8), we used R [R Core Team, 2018] to implement a standard Metropolis-Hastings algorithm with Gaussian proposals reflected into the positive quadrant [Brooks et al., 2011]. Starting locations were chosen by sampling from the prior distribution. Before the usual "burn-in" phase, we included a period of "pre-burn-in" which used the same MCMC procedure with a larger $\sigma_\epsilon$, to allow the chain to more quickly converge on the high-posterior portion of parameter space. Typically, we ran MCMC for $10^6$ iterations of pre-burn-in and $3 \times 10^6$ iterations of burn-in, followed by $4 \times 10^6$ iterations which were used to estimate posterior distributions, which took around 10 hours on a single core of a modern computer with 16 demes. For small graphs fewer iterations were necessary. We used standard methods to assess convergence and mixing.

## Test cases and simulations

We compared inference under coalescence time and resistance distance models using both data from the model and from more realistic simulations. For the first category, we designed a number of graphs to test particular aspects of inference, with migration rates specified on each directed edge (plotted below using igraph [Csardi and Nepusz, 2006]). Given the edge weights ($G$) and the coalescence rates ($\gamma$) of a graph, we produced data by calculating exact coalescence times ($\mathcal{C}(G, \gamma)$), to whose entries we added independent Gaussian noise while preserving symmetry. We scaled the noise to the mean value of the times themselves, so that a "noise level" of $\alpha$ refers to data in which the standard deviation of the noise was set to $\alpha$ multiplied by the average coalescence time across all pairs of populations. Particular parameters and levels of noise are given in the Results. These simulations are expected to be nearly equivalent to neutral, discrete population-based simulations (either forwards-time or coalescent), except that noise terms about the theoretical mean should be somewhat correlated.

**Forwards-time simulations**   To produce realistic data, we implemented forwards-time simulations using SLiM v3.1 [Haller and Messer, 2018, **?**], with individuals living across continuous, two-dimensional geography (sometimes with barriers), from which we recorded genomic data. The basic simulation, which we modified to produce several other situations, is as follows. Each simulation had around 6400 diploid, hermaphroditic individuals, living across two-dimensional geography. Mates were selected from nearby individuals using a Gaussian kernel with standard deviation $\sigma_d$, truncated at $3\sigma_d$. Simulations were done on either a square region with width equal to $80\sigma_d$, or a $5:3$ rectangular region with the same area. Offspring are dispersed away from the mother using the same kernel, reflected from the boundaries of the habitable area. To produce

a realistic model and prevent excessive population clumpiness [Felsenstein, 1975], we model local competition instead of a globally constant population size. To do this, we use the same truncated Gaussian kernel to define an "interaction strength" between each pair of nearby individuals, and compute the probability of survival of each individual to the next time step as $\min(0.9, 2/(1 + 5x/12\pi))$, where $x$ is the sum of the interaction strengths of that individual with all other individuals within distance $3\sigma_d$. (The value $x$ is an estimate of local population density.) This reduces fitness for individuals in denser areas, and produces an equilibrium population density of close to one individual per $\sigma_d^2$ units of area. The probability of survival for individuals within $10\sigma_d$ of the edge of the habitat was multiplied by a linear factor that scaled from 0 to 1 with distance from the edge. Patchiness of the resulting simulations was similar to what is seen in Figure 6.

Each diploid individual has one pair of homologous chromosomes with $10^8$ loci each and a recombination rate of $10^{-8}$ per generation per locus. Neutral mutations were added at a rate of $10^{-9}$ per meiosis. To make these simulations computationally feasible, the mutation rate was set to 0.0 during the forwards simulation, while tree sequences were recorded [?], and mutations were added after the fact with msprime, which is equivalent to including mutations during the forwards simulation but resulted in much faster run times [Kelleher et al., 2018].

To compute genetic distances, geographic space was partitioned into square regions, and within each region, individuals are sampled uniformly for "genotyping" from among those within the middle three quarters of each dimension of the square, as shown for one situation in Figure 6. This protocol was chosen as a compromise between sampling all individuals from near the center of each location, which could result in a large number of close relatives being sampled, and uniform sampling from the whole area of each grid, which may result in many sampled individuals being very close to other grid squares. Mean genetic distances for each pair of regions are then computed as described above. To estimate uncertainty, we computed the standard error of these mean distances using the minimum number of individuals in each location.

Before being passed to the MCMC inference method, we rescaled genetic distances so that the movement rates resulting from the inference would be approximately of order one. We did this by multiplying genetic distances by a constant so that the rescaled mean of the entries of $D$ is equal to the number of locations in the discretization.

## Data from *Populus trichocarpa*

We also applied our method to genotyping data from 423 samples of *Populus trichocarpa* and 8 samples of the closely related *Populus balsamifera* (with which it hybridizes), from a large region of northwestern North America, described in Moreno Geraldes et al. [2014b]. These data include geographical coordinates and genotypes from a genotyping chip targeting 34K SNPs. In addition to preliminary filtering described in Moreno Geraldes et al. [2014b], we additionally removed 2,314 SNPs with more than 5% missing data, retaining 30,756 SNPs, and two individuals, one with more than 15% missing data and one that is much further east than all the other samples. We then computed pairwise divergence between the remaining samples. We discretized the landscape manually into nine regions, preserving species boundaries and choosing divisions along gaps in sampling to keep geographic areas roughly equal. The numbers of samples included in each discretized region varied from 1 to 268, but our method does not assume equal sample numbers (however, an $F_{ST}$-based method would likely be affected by such large differences in sampling).

## Code and data availability

All code used for this work is available at `https://github.com/elundgre/gene-flow-inference` (including an R package that implements the MCMC method) and `https://github.com/petrelharp/isolation_by_coalescence` (including the SLiM simulations). Sequencing data for *Populus* is available from Data Dryad [Moreno Geraldes et al., 2014a].

# Results

## Model validation

We first tested the method using data generated under the model. To test the methods across a wide range of situations, we generated fifty sets of random movement rates on $3 \times 2$ rectangular grids: twenty-five symmetric (i.e., with $G_{ij} = G_{ji}$) and twenty-five asymmetric. We generated movement parameters by rounding independent exponential random variables with mean 1 up to the nearest one tenth, and fixed coalescence rates at 1 for all locations. We then analytically computed mean coalescence times, and added independent noise to each pairwise coalescence time. We assume that we can estimate the amount of noise reasonably well, so used the true standard deviation of the noise for $\sigma_\epsilon$ in the likelihood function. In practice, $\sigma_\epsilon$ can be estimated by the standard deviation of genetic distances between different pairs of samples in the same region. To assess the impact on inference of the number of parameters, we performed inference both with and without the assumption that coalescence rate is the same everywhere. For $3 \times 2$ graphs, there are 21 equations and 14 movement parameters, so that with a global coalescence rate there are 15 unknowns. However, with individual coalescence rates there are 20 unknowns, which is close to nonidentifiable. To quantify accuracy across these random graphs in different situations, we computed, for each model fit on a particular random graph, the absolute difference between the posterior median of each movement parameter and the true value. We then averaged these across movement parameters to produce a measure of accuracy for that model fit, reported below as "mean absolute error".

**Varying noise** Unsurprisingly, coalescence time inference became less accurate as the amount of noise increased. As we varied the standard deviation of the noise from $1/1000^{\text{th}}$ to $1/50^{\text{th}}$ of the mean value of $C$ for that grid, the mean absolute error of inferred gene flow rates ($G_{ij}$) for coalescence time inference with a single coalescence rate increased from around 0.05 to 0.4. Since true values of $G_{ij}$ were of order 1, this is a transition from precise to very rough (but still informative) inference. Posterior interquartile ranges increased proportionally, although there was substantial variation in accuracy between replicates; see Figures S2 and S3. Increasing the number of parameters by allowing multiple coalescence rates made the inference problem much harder – mean absolute errors no longer depended strongly on the amount of noise added, and hovered around 0.4.

More surprisingly, the performance of resistance distance inference did not depend on the amount of noise – mean absolute error was around 0.6 across all levels of noise, both with and without more than one parameter for local diversity (see Figure S2). Although symmetry did not affect coalescence time inference, resistance distance inference did substantially worse on asymmetric graphs, showing median absolute errors of around 0.8 – inferred gene flow rates were almost uncorrelated with true values.

**Varying coalescence rates** Lower coalescence rates mean that lineages wander about the landscape for longer before they coalesce, thus greatly reducing the geographic information we get from coalescence times [Wilkins, 2004]. For instance, if between-population gene flow and coalescence rates are similar, then the lineages of two samples in the same population are likely to coalesce before either leaves, leading to a strong signal of isolation by distance. On the other hand, if coalescence rates are much smaller than gene flow, nearby samples are unlikely to share more recent common ancestors than distant ones. Indeed, coalescence rates had a strong effect on feasibility of the inference problem (shown in Figures S4 and S5): lowering the coalescence rate from 10 to 0.1 (always adding noise with standard deviation $1/200^{\text{th}}$ of the mean value) increased mean absolute error of coalescence time inference from around 0.05 to 0.5. (Gene flow rates are of order 1, so this range of coalescence rates spans strong to weak isolation by distance.) Again, allowing multiple coalescence rates or using resistance distance inference were highly inaccurate in all cases, with mean absolute errors of above 0.5.
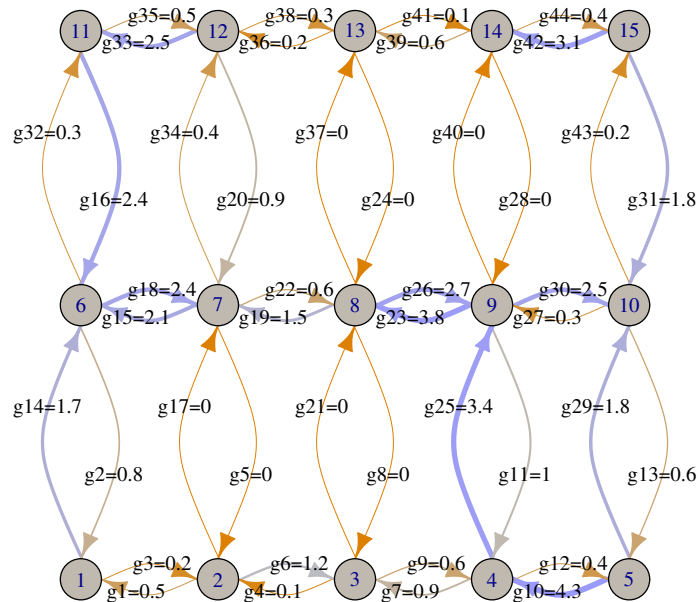
**5x3 Graph with Barriers**



Figure 2: The grid structure and parameter labels for the $5 \times 3$ grid with two barriers: movement rates between $\{2, 3\}$ and $\{7, 8\}$ are zero, as are those between $\{8, 9\}$ and $\{13, 14\}$. Values for the non-zero movement rates were chosen by rounding independent draws of an exponential random variable with mean 1 up to the nearest tenth. Thickness and color of arrows reflect movement rates: darker red arrows have smaller rates and darker blue arrows have larger rates.

## Identifying a barrier to gene flow

We then test the method's ability to locate barriers to migration on the $5 \times 3$ grid with asymmetric gene flow shown in Figure 2. Each nonzero movement rate is determined randomly as before, and coalescence rates are set to 1 everywhere. Figure 3 shows posterior distributions of the movement rates for both coalescence time and resistance distance inference on this graph, with noise standard deviation equal to $1/1000^{\text{th}}$ of the mean coalescence time (top) and $1/100^{\text{th}}$ of the mean coalescence time (bottom). Although increased noise in the data increased uncertainty in the estimated values, coalescence time inference correctly inferred not only the location of the barrier but also the migration rates along all other edges within a reasonable margin of error. Resistance distance inference also identified the barrier, but was much less accurate for the other values. We also explored making the problem harder, by first (a) dropping data corresponding to populations 2, 5, 7, and 15; and then (b) allowing a separate coalescence rate for each location, in both cases using a noise level of $1/100$. The resulting posterior distributions are shown in Figure S6, and show substantially increased error, but only in movement rates to the removed locations. As before, uncertainty was increased when multiple coalescence rates were allowed, but not as strongly as before, likely because the problem is less close to being underconstrained, having 105 equations and 59 unknowns.

## Biased migration

Both matrices of coalescence and commute times, $C$ and $R$, are symmetric, but they do not deal with asymmetric (biased) migration in the same way. Since commute time to location $i$ requires paths both to and from $i$, but coalescence time to $i$ does not, if there is a low rate of migration back into $i$, then commute times to $i$ could be quite long even while coalescence times are not. For instance, suppose there are three
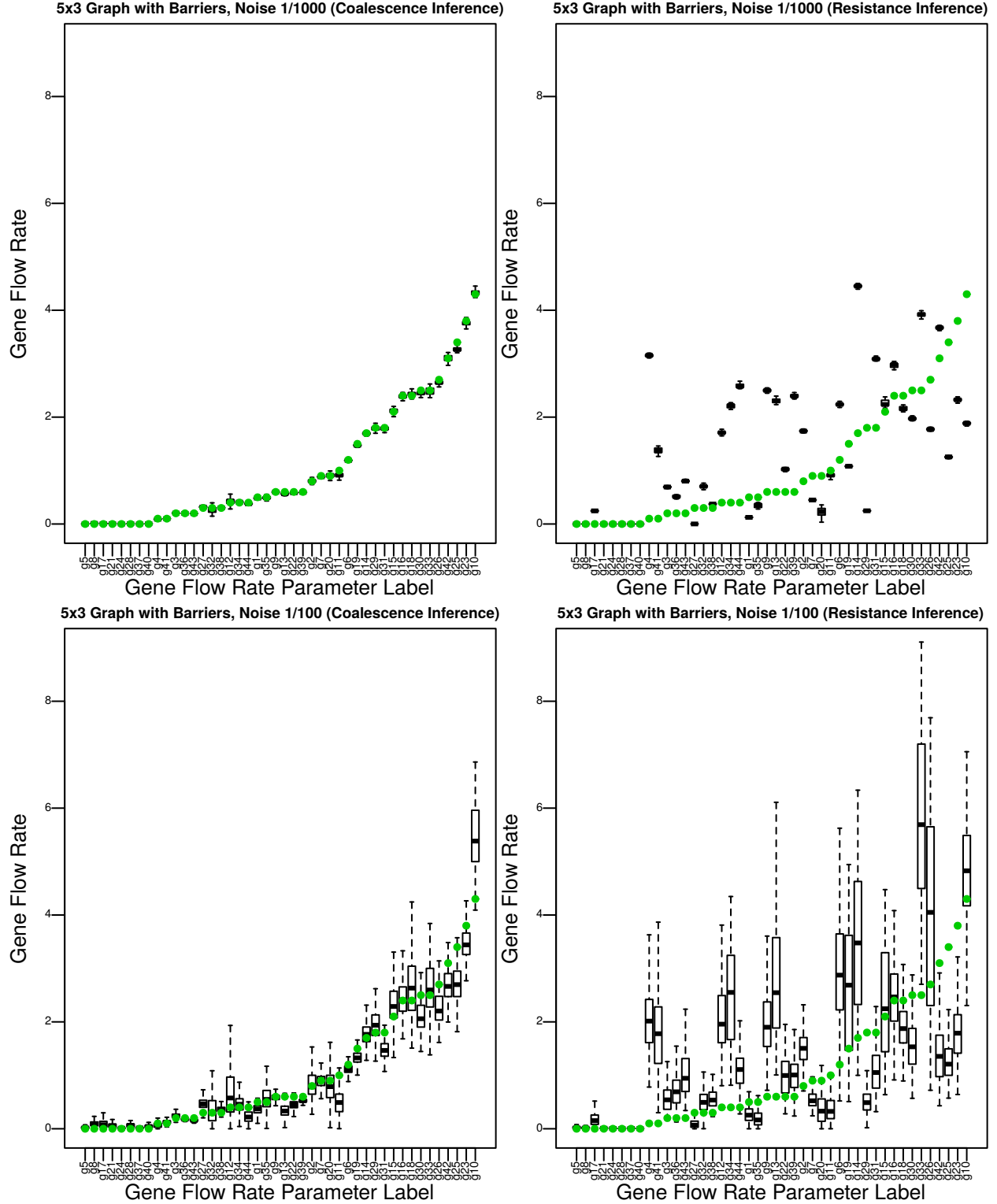
Figure 3: Coalescence time inference is much more accurate than resistance inference: posterior distributions for gene flow rates in the 5 × 3 graph with barriers, compared to true values (in green), using **(left)** coalescence time and **(right)** resistance distance inference, with **(top)** low noise and **(bottom)** high noise, See Figure 2 to match parameter labels to positions on the graph.

populations arranged in a line, and lineages currently in the outer populations are much more likely to come from the central population than the other way around. Since lineages quickly move to the center and coalesce regardless of starting position, coalescence time (and genetic diversity) will be relatively low between all individuals. Commute time between the two outer locations, on the other hand, will be much longer than other comparisons, since it requires a lineage to leave the center.

In order to investigate this general situation, we tested both methods on four different $4 \times 4$ graphs (shown in Figure S7): *uniform*, where all movement rates are 1.0; *symmetric*, where movement rates are symmetric ($G_{ij} = G_{ji}$) and randomly generated as before; *asymmetric*, where all movement rates are random; and *biased*, where movement rates down or to the left are equal to 2.0, and movement rates up or to the right are 0.5. For inference, we added noise with standard deviation $1/500^{\text{th}}$ of the mean value.

Differences between true mean coalescence times ($C$) and mean resistance distances ($\widetilde{R}$) are shown in Figure 4: they are fairly small in the uniform and symmetric cases, moderate in the asymmetric case, and extreme in the biased asymmetric case. This difference suggests that inferences made with resistance distance may be strongly misleading in the asymmetric and biased situations, but in principle it still could be the case that the movement rates that give the best fit of resistance distance to coalescence time data could be close to the actual rates use to generate the data. This does not seem to occur in practice: coalescence time inference was substantially more accurate in all cases. Posterior distributions of inferred movement parameters are shown in Figure 5. The mean absolute errors for coalescence time inference are 0.12 or less in all cases. Resistance distance inference obtains roughly uniform migration rates (although varying by a factor of 2) in the uniform case; and migration rates noisily correlated with the truth in the symmetric graph. However, resistance distance inferences for the asymmetric and biased graphs are only weakly correlated, if at all, to the truth. Resistance distance inference also drastically overestimates movement rates for the biased case, as we would expect based on the differences discussed above.

## Continuous geographical space

The data we have used thus far are produced under the model used for inference, and should provide an accurate depiction of our method applied to discrete, randomly mating populations whose connections by migration are known. However, this is nearly always a rough approximation to reality, in which organisms are distributed across continuous geography, and "populations" are constructed by necessity, often driven by sampling locations. For this reason, we applied coalescence and resistance inference, as well as the resistance-based method EEMS [Petkova et al., 2016], to data from simulations on continuous geography.

**Process noise** The mean coalescence times of lineages that we compute analytically are exact for large, randomly mating populations, but the word "mean" indicates an average across several levels of randomness: each observed, empirical mean estimated using a sample of genotypes will deviate from this depending on the individuals sampled ("individual sampling noise") [Ashander et al., 2018], the genetic loci genotyped ("genome sampling noise") [Waples and Faulkner, 2009], and the stochasticity of the population history itself ("process noise") [Wakeley et al., 2012, Waples and Faulkner, 2009]. Sequencing of many nonascertained loci genome-wide should minimize the second source of noise (although genome structure can affect this at large scales [Li and Ralph, 2019]). Geographic models in continuous space, are expected to show much more process noise than discrete population models because of random fluctuations in local population density. To quantify the relative contributions of the remaining sources of noise, we compared mean genetic distances, calculated in the same way, between two nonoverlapping sets of samples from each of three identical simulations. These forwards-time, continuous-space simulations were done using SLiM as described in the Methods. We found that with these parameter values, process and sampling noise were of similar magnitude, contributing 6.7% and 13.8% of the variance, respectively (Supplemental Figure S8).

**Biased migration** To test inference on a simple, continuous landscape with bias, we simulated a square, flat landscape as above, but with *biased migration*: each offspring's location was chosen randomly as before, but with mean location $\sigma_d/10$ up and to the right of the parent's location. This again produces reverse-time
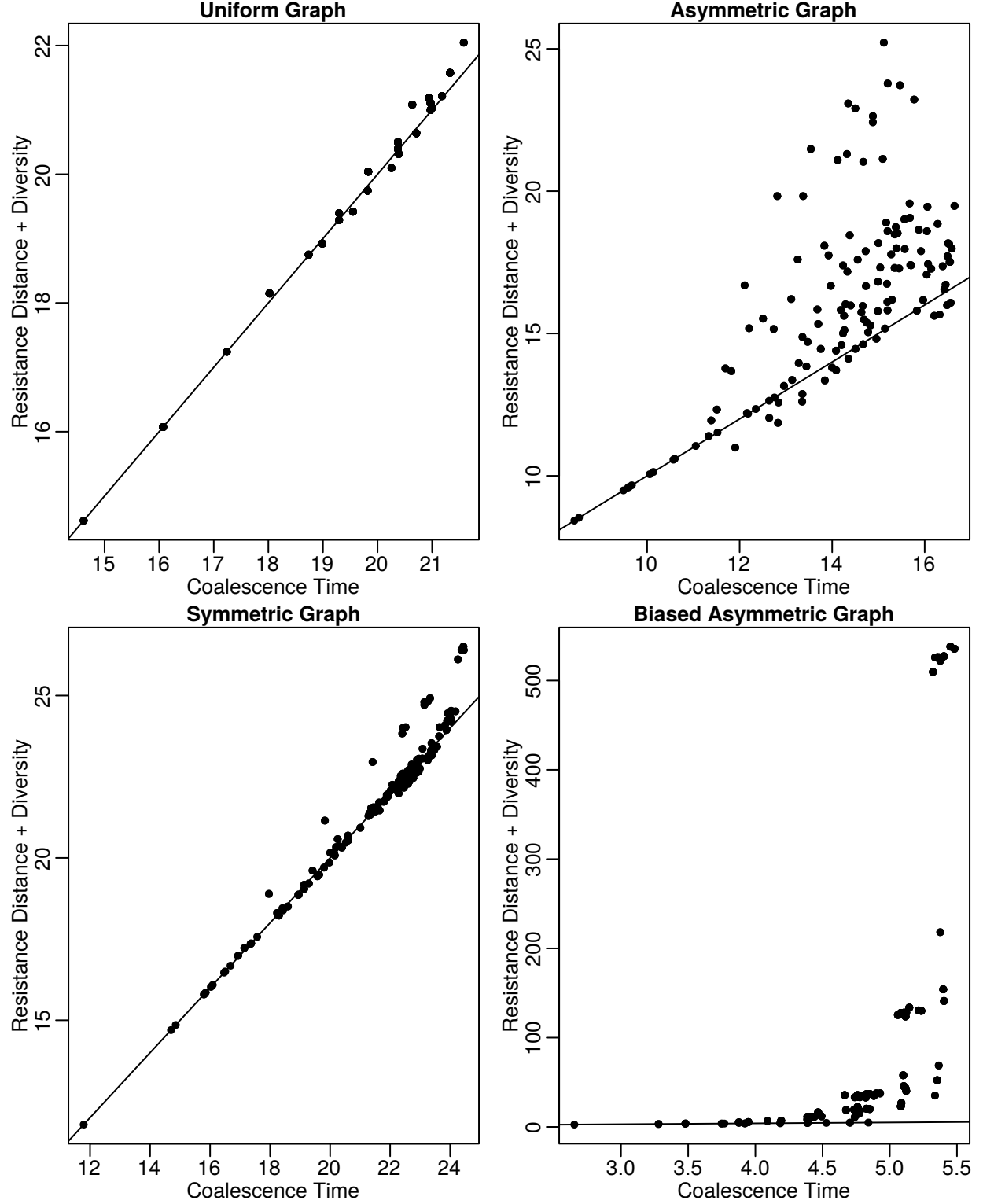
Figure 4: Resistance distances ($\widetilde{R}$) compared to coalescence times ($C$) on the $4 \times 4$ graph, with **(top left)** uniform movement rates, **(bottom left)** random, symmetric rates, **(top right)** random, asymmetric rates, and **(bottom right)** rates with a small diagonal bias (see text). The line shows $y = x$. See Figure S7 for specific values and graph structure.
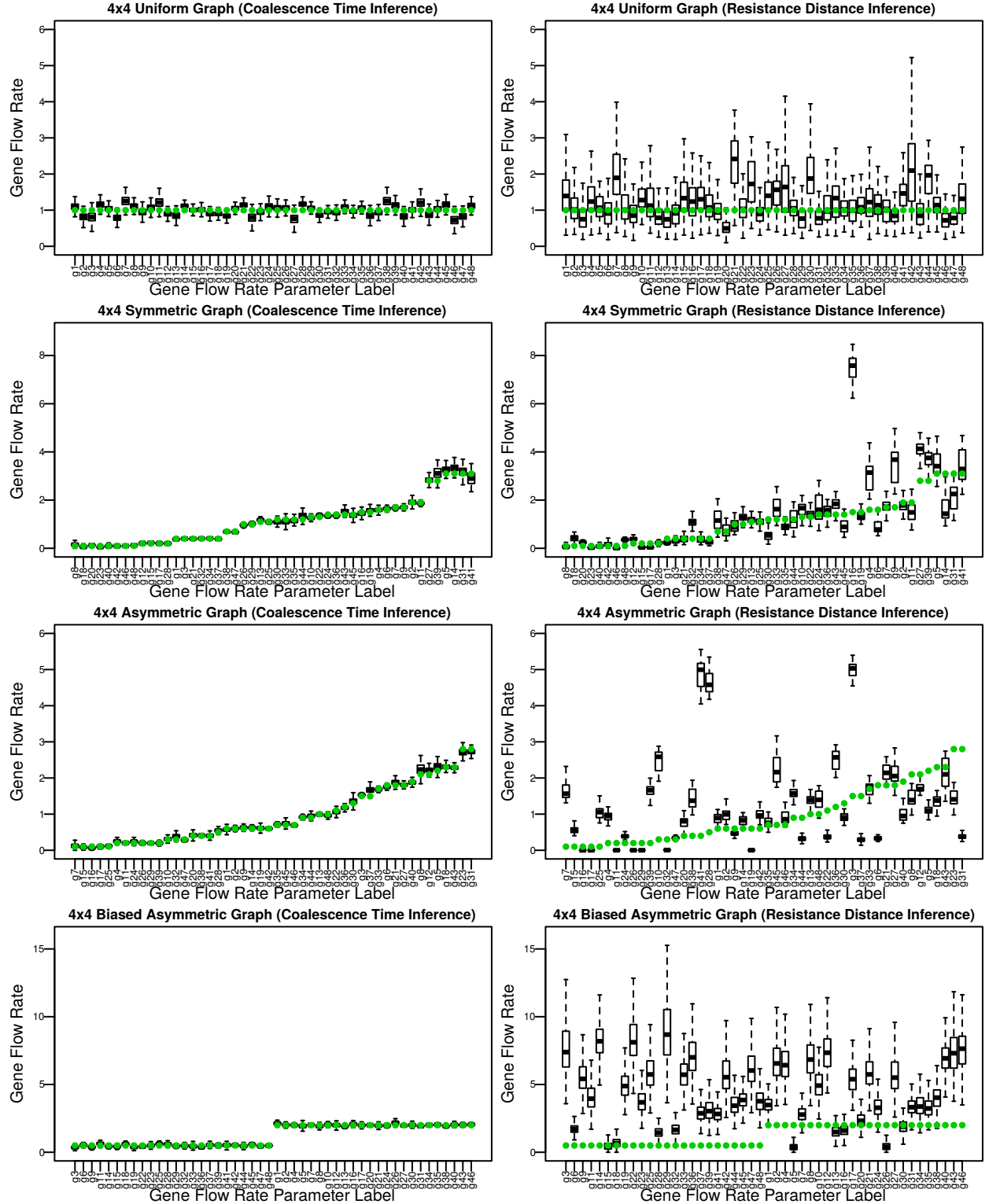
13

Figure 5: Boxplots of the posterior distributions of movement rates inferred using the **(left)** coalescence times and **(right)** resistance distances shown in Figure 4; i.e., on the $4 \times 4$ graphs with **(top)** uniform, **(middle top)** symmetric, **(middle bottom)** asymmetric, and **(bottom)** biased movement rates. See Figure S7 for specific values and graph structure.

14

gene flow down and to the left. Coalescence time inference correctly infers the bias on a broad scale: using a $4 \times 4$ grid, inferred gene flow rates down and to the left are consistently much larger than those up and to the right; resistance distance-based results show no clear pattern (Supplemental Figure S10). However, we do not obtain the clear picture of the landscape we saw for the corresponding discrete-population model (bottom-right plot, Figure 5): inferred rates show substantial heterogeneity, likely due to stochasticity of recent demography.

**Identifying a barrier**   We now revisit the earlier situation where a landscape has locations that are barriers to gene flow. The landscape is shown in Figure 6, where red bars depict uninhabitable regions that block migration. Since the distribution of offspring locations is truncated at three standard deviations away from the mother, a sufficiently thick uninhabitable area completely stops migration directly across it. We calculate mean genetic distances using 50 individuals from each grid location, here giving us a total of 750 individuals. The gene flow rates across the barriers are reliably estimated to be very small, while other values have substantial variation: in particular, gene flow rates are estimated to be low across some edges that do not cross barriers; this may be because of recent demographic stochasticity. The barriers were also identified with comparable accuracy by both our resistance distance method and EEMS, as shown in Supplemental Figure S11. Note also that this analysis began by grouping samples into discrete "populations" appropriately; in absence of a good *a priori* idea of where barriers are, this step might not be straightforward. To make parameters most easily interpretable, geography should probably be discretized along natural barriers and so that each region is of roughly the same geographic area.

**Other barriers: population sinks and recent expansions**   We simulated two other situations on a continuous landscape that produced an bias in effective migration. First, we simulated a **valley** in a square landscape, in which fecundity of individuals in the middle 1/4 of the landscape was reduced by 50%. The valley is a population "sink", although it would not be detectable with mortality rates, and shows only a slightly lower population density (Supplemental Figure S12). Since individuals in the valley are more likely to have parents outside of the valley, this produces gene flow "uphill", away from the ridge. Next, we simulated a recent **expansion**, in which the middle 4/5 of the landscape was uninhabitable for 400,000 generations, until 500 generations before the present day. (This is a model of secondary contact with a long period of isolation, but not outside the realm of possibility.) The resulting expansion produces gene flow back away from the center, similar to the "valley".

Both coalescence time inference and the resistance landscape inferred by EEMS show a barrier to gene flow in the middle of the landscape (Figure 7). This is arguably correct, although there is in fact no current barrier to migration in either simulation. Coalescence time inference also correctly infers the general bias in recent gene flow away from the center, although as in other continuous-space simulations, there was substantial noise in the inferred patterns. However, the resistance landscapes as inferred by EEMS show patchy, vertical bands of high resistance. These patterns are commonly seen when attempting to use EEMS, whose underlying model of gene flow is symmetric, to describe anisotropic gene flow. The grid-like pattern visible in this and other EEMS results may be due to the sampling scheme (recall that samples are drawn from the middle three-quarters of each grid square). Our analysis above shows that this is an unavoidable consequence of the resistance approximation, and our implementation of resistance distance inference, which allows asymmetric gene flow, shows similar patterns (Supplemental Figures S12 and S13).

# Application to *Populus*

Our discretization of the sampling area for the two poplar species is shown in Figure 8, along with arrows depicting posterior mean estimates of gene flow. Posterior distributions of gene flow rates and coalescence rates are shown in Supplemental Figures S14 and S15. The main features of the resulting model are: (a) low but nonzero gene flow between species, with the highest rate between regions 3 and 4; (b) strong bias in gene flow among (inland) *balsamifera* regions, from southeast to northwest ($3 \to 5 \to 6 \to 1$); and (c) strong bias in gene flow into regions 2 and 8. These results align with what is known about *Populus* history and
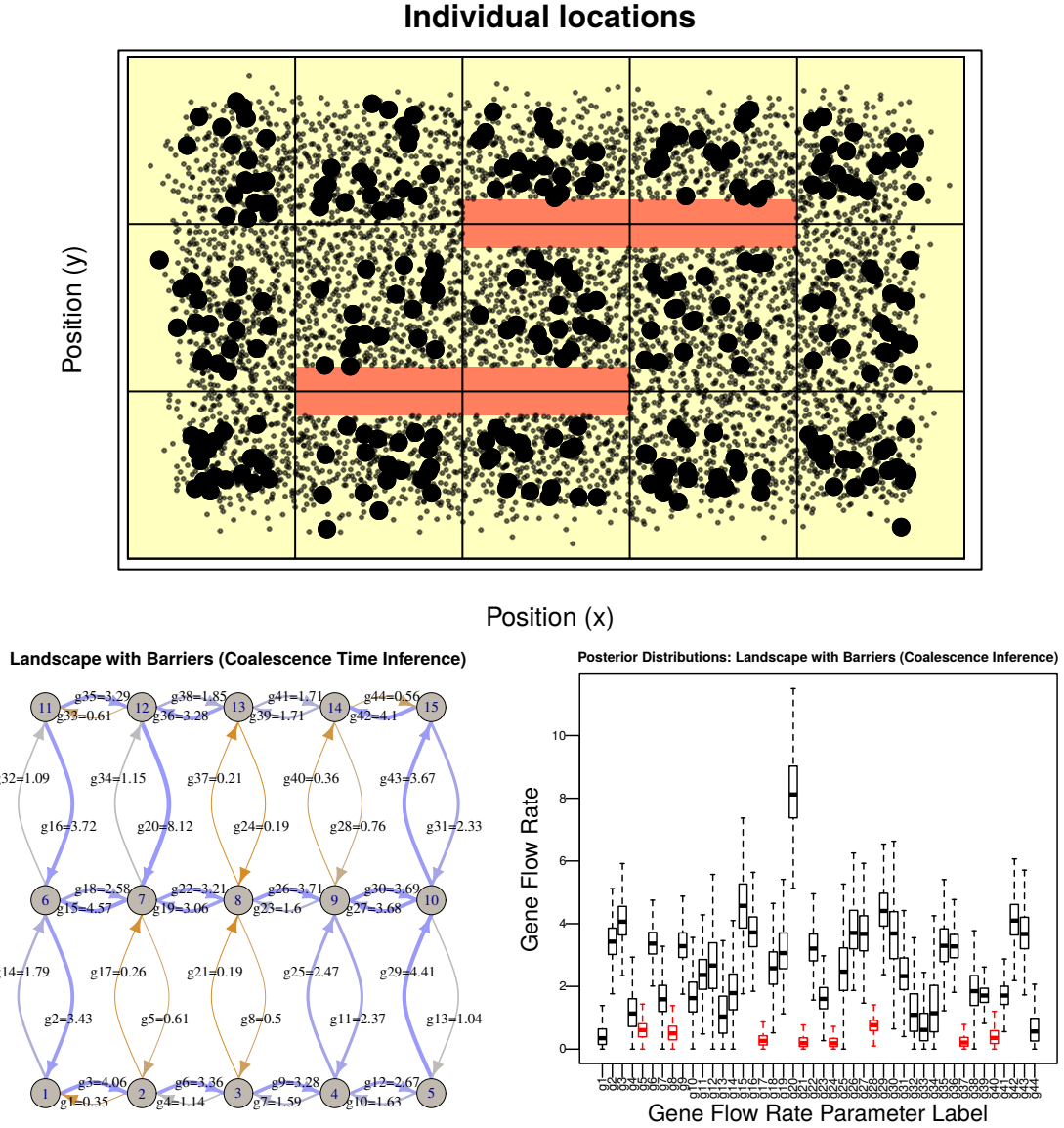
Figure 6: **(top)** Locations of individuals on the $5 \times 3$ landscape with barriers, with individuals used to compute the mean genetic distance matrix marked in bold. Red bars show uninhabitable regions, which are sufficiently thick so that no migration can occur directly across them. **(bottom left)** Posterior medians of movement rates inferred using coalescence time inference, and **(bottom right)** boxplots of corresponding posterior distributions, with movement rates crossing the barriers colored in red. The grouping of individuals into a $5 \times 3$ grid is shown above, and labels are the same as in Figure 2.
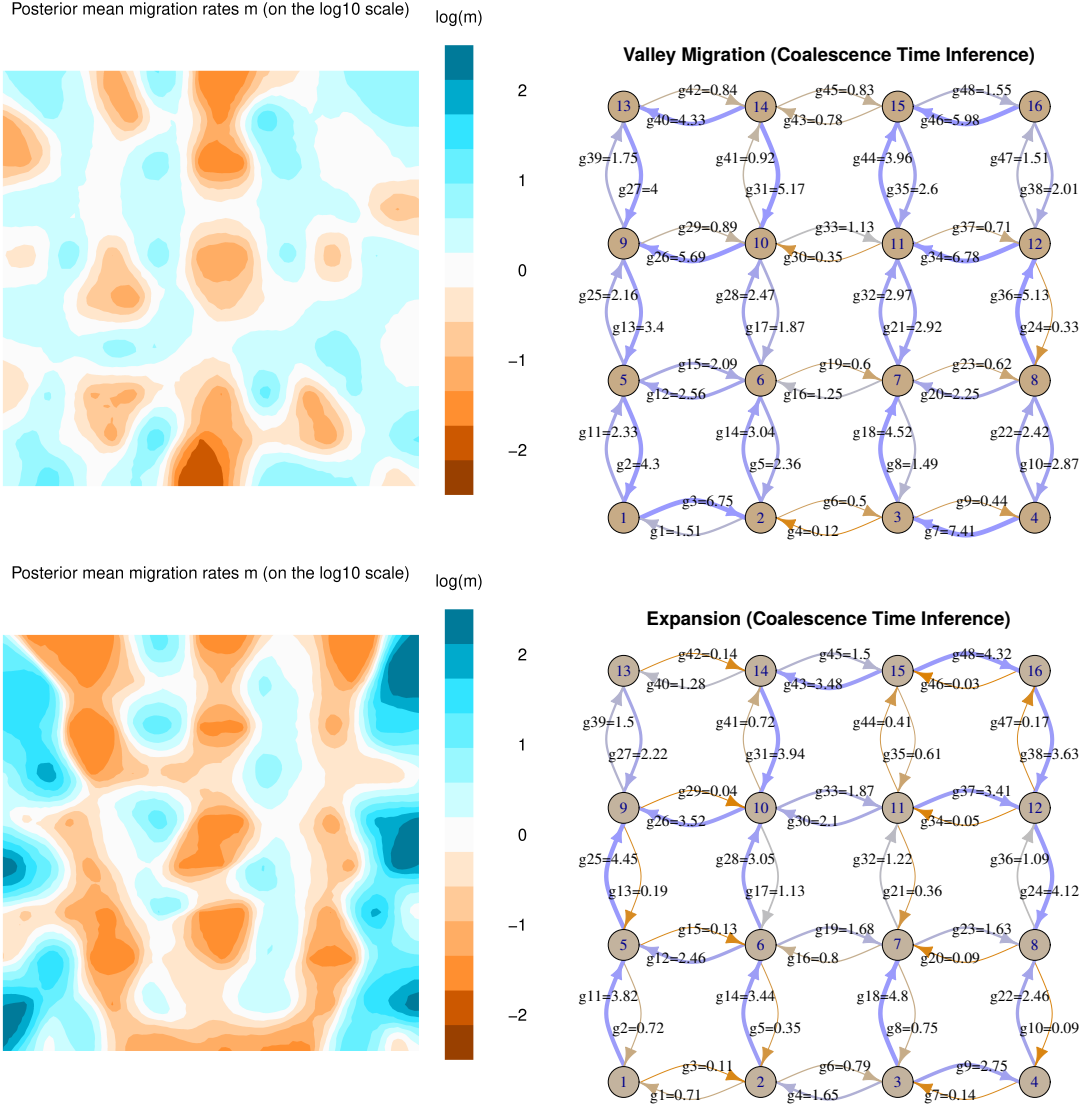
Figure 7: **(Left:)** resistance landscapes inferred by EEMS and **(right:)** gene flow rates inferred using coalescence time inference, from individual-based simulations on a continuous landscape, with **(top)** a *valley* of reduced fecundity in the middle, and **(bottom)** a recent *population expansion* from both edges of the range that met in the middle. The color scale shows the posterior mean log migration rates inferred by EEMS.

ecology in the region (personal communication, A. Moreno Geraldes and Q. Cronk, and Moreno Geraldes et al. [2014b]). There is ongoing hybridization around region 4, and interspecific gene flow from 9 to 3 may be due to downstream transport along the Columbia river (a larger gene flow rate from 9 to 3 indicates that individuals in region 9 are more likely to have recent ancestry in region 3 than vice-versa.) The glacial refugia for the two species are thought to be in western Alaska (*balsamifera*) and coastal British Columbia (*trichocarpa*). Inferred gene flow leading back towards these regions (depicted by larger arrows on the map) are consistent with this – for instance, if region 5 was colonized from region 6 sufficiently recently, then individuals in region 5 should trace their ancestry to region 6 much more frequently than vice-versa, as indicated by the large $5 \rightarrow 6$ arrow and small $6 \rightarrow 5$ arrow in Figure 8.

Interpreting these results requires some nuance beyond what was necessary in our simulation results. Sampling locations are sparse, especially in the inland species, so how exactly should we think of the geographic extent of "region 6", which is represented by only two, distant samples? Is this region's low inferred coalescence rate a result of simply a large population (due to a large geographic region) or barriers to movement within the region? Although it is not entirely clear how to translate discrete-population models to continuous space, a "gene flow rate" from region $i$ to region $j$ as shown in Figure 8 is best thought of as an estimate of the proportion of the individuals in region $i$ that have a parent in region $j$, averaged over time and scaled by some unknown factor. Equivalently, this is the probability per unit time that a lineage traced back from an individual in region $i$ follows a line of descent to region $j$, again scaled by some factor. We therefore expect gene flow to be biased from an area of lower population density (or, net fecundity) into a neighboring region of higher population density. We also expect gene flow to be biased from a smaller region to a larger, neighboring one than vice-versa if a larger proportion of the smaller region lies close to the boundary between the two. This may explain the net bias from many coastal populations to inland ones. We grouped samples so that each group represented roughly comparable geographic regions, to ameliorate these confounding factors. However, these difficulties in interpretation are common in any situation where discrete populations are used to model continuous geography.

# Discussion

In this paper, we study how to use genetic and geographic distances between present-day samples to infer the demographic parameters of a population that lives across a heterogeneous two-dimensional landscape. In particular, we have shown that the resistance distance approximation – which underlies several of the most commonly-used tools of landscape genetics – can produce erroneous estimates, especially in the presence of biased gene flow. We implement an alternative method, which uses coalescence times instead of the resistance distance approximation, which provides good estimates of gene flow in a wider range of situations (Figures 3 and 5). This weakness of resistance-based methods is not surprising – the original papers describing Circuitscape [McRae, 2006] and EEMS [Petkova et al., 2016] present the resistance approximation as a necessary step for computational feasibility. Results of resistance-based methods should therefore be interpreted with caution: for example, high inferred gene flow between two areas may actually mean the areas are being fed by a common source.

Our new method infers effective population sizes and gene flow rates quite well – and, being Bayesian, provides estimates of uncertainty – given data from discrete populations connected by migration. Can our method replace resistance-based methods? Perhaps, but the substantial uncertainty we saw on graphs with only tens of nodes is indicative of a larger problem we face for realistic models. We have seen that discretization of space results in substantial modeling error, in part because of randomness of geographic sampling and unmodeled process noise can lead to overfitting. Partitioning space into a finer grid should help with these problems, but tends to make the inference problem itself more ill-conditioned: with more connections, changing the value of one connection affects coalescence time less, and so inferences about that value must necessarily be less certain. This tradeoff implies some degree of unavoidable uncertainty. Reproducible, reliable inference will likely require development of new inference methods that explicitly model continuous geography. In the meantime, comparison of results utilizing different discretizations of geography can help identify problems.
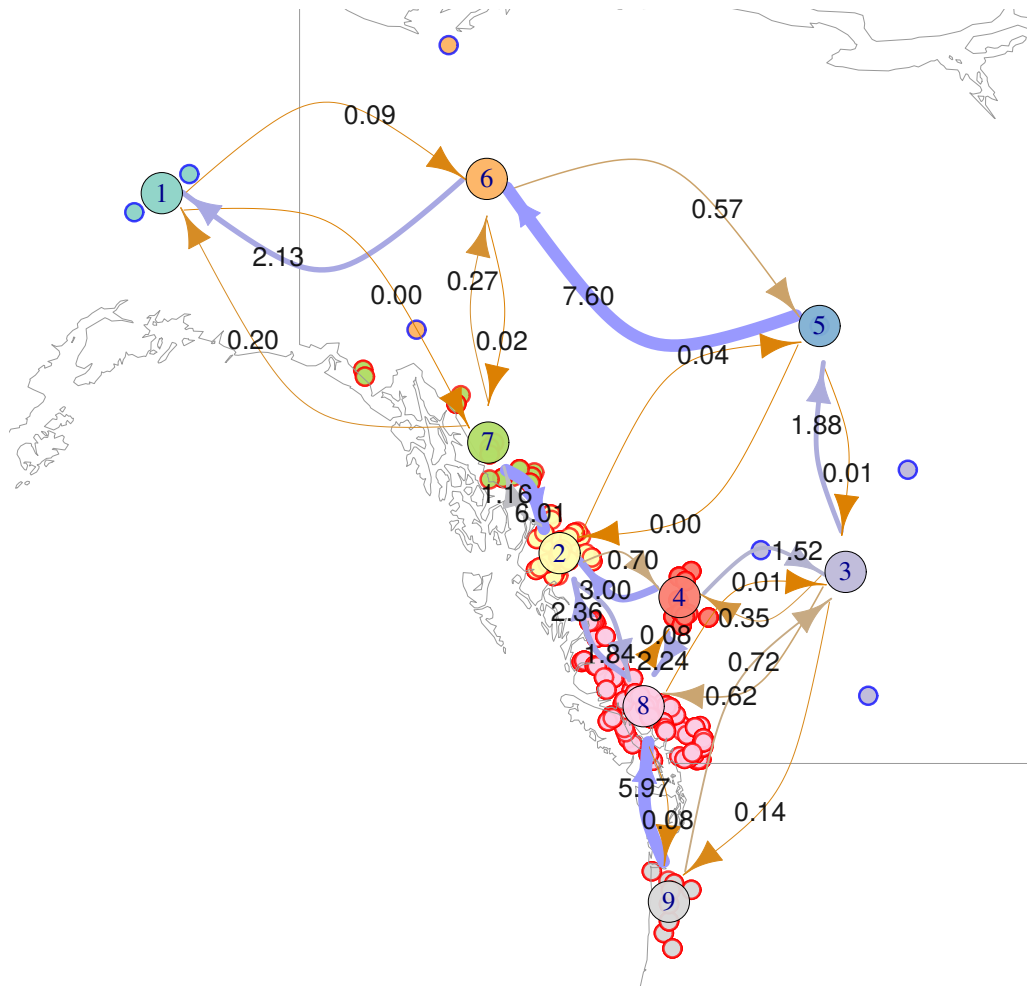
18

Figure 8: Model results for *Populus* data, superimposed on a map of northwestern North America. Sampling locations of *Populus* genomes are small circles, with outer color indicating species (red-outlined, coastal samples are *trichocarpa*, blue-outlined, inland samples are *balsamifera*); circle fill color indicates how samples are grouped into discrete "populations". Large circles are placed at group centroids, and given group labels. Arrows are labeled by the posterior mean gene flow rate inferred under the coalescence time model (which also determines arrow width and color). For instance, the inferred gene flow rate from 4 to 2 is 3.0, while that from 2 to 4 is 0.7, suggesting that poplars in region 4 have many more recent ancestors in region 2 than poplars in region 2 do in region 4. Northwestern bias in gene flow between *balsamifera* regions may reflect postglacial expansion to the south and east out of a refugium in Alaska.

Although commute and coalescence times can be quite different, they are equal (with a particular choice of local diversity) if populations are arranged on a ring or torus with symmetric migration (as also noted by McRae [2006]). The similarity of these models to rectangular grids may explain why in other work, resistance distance methods have shown relatively good fit to data simulated with symmetric migration rates.

**Other methods** For comparison on equal footing, we have implemented a resistance-based inference method. However, methods that use resistance distance have substantial advantages over the method we present here. Circuitscape [McRae et al., 2008] produces maps of much higher resolution than is presently possible with coalescent times. Hanks and Hooten [2013] connects the problem to intrinsic conditional autoregressive models, providing a Bayesian model of an underlying Gaussian Markov random field. EEMS [Petkova et al., 2016] integrates over possible tessellations of the region as a way of regularizing the inferred landscape, aiming to obtain a map at the best possible resolution supported by the data.

Most promisingly, the recent method, MAPS ["Migration and Population Surface estimation", Al-Asadi et al., 2018] is based on EEMS, but instead of resistance distances, uses pairwise sharing of long haplotype segments, which have been shown to carry substantial information about recent demography [Ralph and Coop, 2013, Palamara and Pe'er, 2013, Browning and Browning, 2015, Ringbauer et al., 2017]. Furthermore, the likelihood model underlying MAPS is based on coalescent theory, and thus should not be subject to the drawbacks of resistance distance. Ringbauer et al. [2018] also uses shared haplotype lengths to identify a barrier in a coalescence-based framework. However, the underlying migration model is symmetric, and haplotype length-based methods require fairly dense genotyping and a genetic map, something not available for many species.

Other widely-used inference methods, such as MIGRATE [Beerli and Felsenstein, 1999, Beerli and Palczewski, 2010], BayesAss [Wilson and Rannala, 2003], and IMa [Hey and Nielsen, 2007] use likelihoods for the joint frequency spectrum derived from a coalescent model – and so in principle could use much more of the data than our method, which only uses pairwise divergences. However, because they use locus-specific data rather than an average across loci, these methods can only be applied to a relatively small number of populations and loci, because of computational efficiency. We have found asymmetry in migration rates to be important: Hanks [2017] developed a method that allows asymmetry by modeling genetic similarity as deriving from an underlying random field whose space-time covariance is given by the covariance of the (forwards-time) population fluctuations. However, this is not motivated by a generative model for genetic data.

All of the methods presented above work with a discretized model of space, for mathematical and computational reasons. Development of new methods for continuous geography and assessment of how current methods behave when faced with continuous geography is an important challenge facing the field. This has been made substantially easier with the introduction of continuous space into the simulator, SLiM [Haller and Messer, 2018], that we used to test the behavior of our method with more realistic data. Another promising approach centers around the Spatial Lambda-Fleming-Viot model [Barton et al., 2010], which provides a mechanistic model in which coalescent simulations are possible. This has been used for inference [Guindon et al., 2016], but more work remains to understand how it behaves as an approximation to real populations.

**Asymmetric dispersal and consequences for resistance methods** We have found that asymmetric rates of lineage movement can produce qualitative differences between coalescence times and resistance distances, and thereby mislead models based on resistance distance. How should this affect the results of resistance-based methods to genomic data, besides general inaccuracy? This asymmetry occurs if one region receives a greater proportion of each new generation as migrants from another population than that other population does from it. This is expected, for instance, if organismal dispersal is biased by wind or water currents [Gaines et al., 2003, Morrissey and de Kerckhove, 2009], or in the presence of source-sink dynamics [Dias, 1996, Lenormand, 2002]. Suppose, for instance, that seed dispersal for a species of tree is biased downhill, and the landscape is dominated by a large valley. Since lineages tend to move uphill, genetic distance between locations on opposite slopes of the valley will be relatively large, so resistance methods will

infer a barrier along the bottom of the valley when no barrier to dispersal exists. On the other hand, if there is a ridge instead of a valley, resistance methods will show no barrier (and relatively high movement rates), even if there is very little uphill dispersal. This could lead to a falsely high assessment of gene flow across the top of the ridge.

**Circuitscape**   Could we use coalescence time in place of commute time for workflows that compute values on a given map of movement rates that are then compared to genetic distance? In principle this could be done, but there is no clear way to do this at the same (impressively fine) geographic resolution that is currently possible, e.g., using Circuitscape [McRae, 2006]. This is because if we have $n$ sampled locations on a landscape discretized into $N$ regions, the computational complexity of finding commute times is $nN$, but coalescence time scales as $N^2$ (Each $N$-vector of hitting times to a particular location can be found independently, but the entire $N \times N$ matrix of coalescence times must be found together.) However, as we discuss above, this fine geographic resolution is in some sense illusory – for each fine-resolution map there should be coarser maps that give almost identical coalescence times – but we are not aware of existing theory providing guidance on how to find these.

**Difficulty of inference**   What determines the feasibility of inferring movement rates from genetic distances? Using coalescence times instead of commute times greatly improves accuracy in many situations, but there are still a number of factors that determine the tractability of the problem. Observation noise is clearly an issue: we found that estimation errors of a few percent was enough to seriously degrade accuracy. However, genetic distances can be estimated to much higher accuracy using modern genomic data. Perhaps more seriously, a low rate of coalescence relative to movement can also make the problem essentially non-identifiable. This is clear at least in the limit: with very low coalescence, the population loses any isolation by distance and is indistinguishable from a randomly mating population. In continuous landscapes, this balance is measured by Wright's local effective population size, which is proportional to the number of other individuals within a circle of radius equal to the mean dispersal distance.

Inference of movement rates, in either a coalescence time or resistance distance framework, is an ill-conditioned problem, implying the need for regularization to obtain reliable inference. This fact could explain the results of Graves et al. [2013], who found a large area of resistance parameters that produced equivalently good fits to genetic distance (i.e., nonidentifiability, analogous to a flat likelihood surface). An anonymous reviewer suggested that although inference of landscapes of movement rates may carry a degree of unavoidable uncertainty, the problem of *model comparison* (e.g., between models with and without migration across a certain barrier) may still produce more certain answers.

Computation time currently limits this method to a discretization of less than 30 populations, but nonidentifiability is probably a more serious barrier that must be concurrently addressed before scaling the method to finer discretizations of space. Finer discretizations of space should benefit from the use of sparse matrix methods, but in our testing these did not speed up computation at this scale.

**The effect of history**   The models we discuss here assume that population sizes and migration rates have been constant on the time scale given by the within-species coalescent time. This is rarely true in practice [Neigel et al., 1991, Barton and Wilson, 1995]. However, geographic differences in mean relatedness are established on a shorter time scale – the time scale over which a lineage, moving randomly across the landscape, "forgets" where it started (i.e., the mixing time of the Markov chain [Wilkins, 2004]). This is the time it takes for the uncertainty in lineage movement to reach the scale of the species range. For instance, if the width of a species' range is roughly 500km, and if mean dispersal distance is 10km, the standard deviation of ancestor location $t$ generations ago is $10\sqrt{t}$, so the mixing time of a lineages across the landscape, not accounting for barriers, is of order 2500 generations. The habitat of many species would have changed substantially over this time, which suggests that models incorporating change over time may be required to model modern diversity. However, the effects of recent history are strongest, so landscapes estimated assuming constant populations may give a reasonable picture of the landscape averaged over recent times.

**Assumptions** Modeling lineages as a Markov chain is nearly ubiquitous in population genetics today, but may not be appropriate. Even if the population dynamics in forwards time are Markov, the dynamics of lineages traced back in time (the coalescent process) may not be. For example, if individual fecundity is variable and population density is low, two lineages near each other are more likely to share a recent common origin, so knowing how one lineage moves is informative about how the other lineage is likely to move. This effect becomes small as population density increases, so it should be a relatively minor point if the offspring of any one parent are typically interspersed with the offspring of many others. Natural selection also makes the coalescent process non-Markovian. Differences in the strength of linked selection along the genome could even cause the statistical behavior of lineages to depend on the region of the genome being studied [Wang and Bradburd, 2014, Li and Ralph, 2019]. However, more investigation with continuous-space models is needed.

# Acknowledgements

# References

Hussein Al-Asadi, Desislava Petkova, Matthew Stephens, and John Novembre. Estimating recent migration and population size surfaces. *bioRxiv*, 2018. doi: 10.1101/365536. URL https://www.biorxiv.org/content/early/2018/07/09/365536.

David Aldous and James Allen Fill. Reversible Markov chains and random walks on graphs, 2002. Unfinished monograph, recompiled 2014, available at http://www.stat.berkeley.edu/~aldous/RWG/book.html.

Jaime Ashander, Peter Ralph, Evan McCartney-Melstad, and H. Bradley Shaffer. Demographic inference in a spatially-explicit ecological model from genomic data: a proof of concept for the Mojave Desert Tortoise. *bioRxiv*, 2018. doi: 10.1101/354530. URL https://www.biorxiv.org/content/early/2018/06/23/354530.

N. H. Barton and I. Wilson. Genealogies and Geography. *Philosophical Transactions of the Royal Society of London. Series B: Biological Sciences*, 349(1327):49–59, 1995. doi: 10.1098/rstb.1995.0090. URL http://rstb.royalsocietypublishing.org/content/349/1327/49.abstract.

Nick Barton, Alison Etheridge, and Amandine Véber. A new model for evolution in a spatial continuum. *Electronic Journal of Probability*, 15:162–216, 2010. URL http://ejp.ejpecp.org/article/view/741.

Peter Beerli and Joseph Felsenstein. Maximum-likelihood estimation of migration rates and effective population numbers in two populations using a coalescent approach. *Genetics*, 152(2):763–773, June 1999. URL https://www.ncbi.nlm.nih.gov/pubmed/10353916.

Peter Beerli and Michal Palczewski. Unified framework to evaluate panmixia and migration direction among multiple sampling locations. *Genetics*, 185(1):313–326, May 2010. doi: 10.1534/genetics.109.112532. URL https://www.ncbi.nlm.nih.gov/pubmed/20176979.

Rajendra Bhatia and Peter Rosenthal. How and why to solve the operator equation AX-XB = Y. *Bulletin of the London Mathematical Society*, 29(1):1–21, 1997. doi: 10.1112/S0024609396001828. URL `http://blms.oxfordjournals.org/content/29/1/1.abstract`.

Steve Brooks, Andrew Gelman, Galin Jones, and Xiao-Li Meng. *Handbook of Markov chain Monte Carlo*. CRC press, 2011.

Sharon R. Browning and Brian L. Browning. Accurate non-parametric estimation of recent effective population size from segments of identity by descent. *The American Journal of Human Genetics*, 97(3):404 – 418, 2015. ISSN 0002-9297. doi: http://dx.doi.org/10.1016/j.ajhg.2015.07.012. URL `http://www.sciencedirect.com/science/article/pii/S0002929715002888`.

Hugo Cayuela, Quentin Rougemont, Jérôme G. Prunier, Jean-Sébastien Moore, Jean Clobert, Aurélien Besnard, and Louis Bernatchez. Demographic and genetic approaches to study dispersal in wild animal populations: A methodological review. *Molecular Ecology*, pages 1–35, 2018. doi: 10.1111/mec.14848. URL `https://onlinelibrary.wiley.com/doi/abs/10.1111/mec.14848`.

Gabor Csardi and Tamas Nepusz. The igraph software package for complex network research. *InterJournal*, Complex Systems:1695, 2006. URL `http://igraph.org`.

Samuel A Cushman, Kevin S McKelvey, Jim Hayden, and Michael K Schwartz. Gene flow in complex landscapes: testing multiple hypotheses with causal modeling. *Am Nat*, 168(4):486–499, October 2006. doi: 10.1086/506976. URL `https://www.ncbi.nlm.nih.gov/pubmed/17004220`.

Paula C. Dias. Sources and sinks in population biology. *Trends in Ecology & Evolution*, 11(8):326 – 330, 1996. ISSN 0169-5347. doi: https://doi.org/10.1016/0169-5347(96)10037-9. URL `http://www.sciencedirect.com/science/article/pii/0169534796100379`.

Peter G Doyle and J Laurie Snell. Random walks and electric networks, 2006. URL `http://arxiv.org/abs/math/0001057`.

Charles L. Epstein and John Schotland. The bad truth about Laplace's transform. *SIAM Review*, 50(3): 504–520, 2008. ISSN 0036-1445. doi: 10.1137/060657273. URL `http://dx.doi.org/10.1137/060657273`.

William Feller. Generalized second order differential operators and their lateral conditions. *Illinois J. Math.*, 1:459–504, 1957. ISSN 0019-2082.

Joseph Felsenstein. A pain in the torus: Some difficulties with models of isolation by distance. *The American Naturalist*, 109(967):359–368, 1975. ISSN 00030147. URL `http://www.jstor.org/stable/2459700`.

Steven D. Gaines, Brian Gaylord, and John L. Largier. Avoiding current oversights in marine reserve design. *Ecological Applications*, 13(sp1):32–46, 2003. doi: 10.1890/1051-0761(2003)013[0032:ACOIMR]2.0.CO;2. URL `https://esajournals.onlinelibrary.wiley.com/doi/abs/10.1890/1051-0761%282003%29013%5B0032%3AACOIMR%5D2.0.CO%3B2`.

Tabitha A. Graves, Paul Beier, and J. Andrew Royle. Current approaches using genetic distances produce poor estimates of landscape resistance to interindividual dispersal. *Molecular Ecology*, 22(15):3888–3903, 2013. doi: 10.1111/mec.12348. URL `https://onlinelibrary.wiley.com/doi/abs/10.1111/mec.12348`.

Stéphane Guindon, Hongbin Guo, and David Welch. Demographic inference under the coalescent in a spatial continuum. *Theoretical Population Biology*, 111:43 – 50, 2016. ISSN 0040-5809. doi: http://dx.doi.org/10.1016/j.tpb.2016.05.002. URL `http://www.sciencedirect.com/science/article/pii/S0040580916300181`.

Benjamin C Haller and Philipp W Messer. SLiM 3: Forward genetic simulations beyond the Wright-Fisher model. *Molecular Biology and Evolution*, page msy228, 2018. doi: 10.1093/molbev/msy228. URL `http://dx.doi.org/10.1093/molbev/msy228`.

23

Ephraim M. Hanks. Modeling spatial covariance using the limiting distribution of spatio-temporal random walks. *Journal of the American Statistical Association*, 112(518):497–507, 2017. doi: 10.1080/01621459. 2016.1224714. URL https://doi.org/10.1080/01621459.2016.1224714.

Ephraim M. Hanks and Mevin B. Hooten. Circuit theory and model-based inference for landscape connectivity. *Journal of the American Statistical Association*, 108(501):22–33, 2013. doi: 10.1080/01621459.2012. 724647. URL http://dx.doi.org/10.1080/01621459.2012.724647.

Jody Hey and Rasmus Nielsen. Integration within the Felsenstein equation for improved Markov chain Monte Carlo methods in population genetics. *Proc Natl Acad Sci U S A*, 104(8):2785–2790, February 2007. doi: 10.1073/pnas.0611164104. URL https://www.ncbi.nlm.nih.gov/pubmed/17301231.

William G Hill. Effective size of populations with overlapping generations. *Theor Popul Biol*, 3(3):278–289, September 1972. URL https://www.ncbi.nlm.nih.gov/pubmed/4667087.

Richard R. Hudson. The variance of coalescent time estimates from DNA sequences. *Journal of Molecular Evolution*, 64(6):702–705, 2007. ISSN 0022-2844. doi: 10.1007/s00239-006-0261-1. URL http://dx.doi. org/10.1007/s00239-006-0261-1.

Jerome Kelleher, Kevin R. Thornton, Jaime Ashander, and Peter L. Ralph. Efficient pedigree recording for fast population genetics simulation. *PLOS Computational Biology*, 14(11):1–21, 11 2018. doi: 10.1371/ journal.pcbi.1006581. URL https://doi.org/10.1371/journal.pcbi.1006581.

John G. Kemeny and J. Laurie Snell. *Finite Markov Chains*. Undergraduate Texts in Mathematics. Springer New York, 1983. ISBN 9780387901923.

James R. Kuttler and Vincent G. Sigillito. Eigenvalues of the Laplacian in two dimensions. *SIAM Review*, 26(2):163–193, April 1984. doi: 10.1137/1026033. URL https://doi.org/10.1137%2F1026033.

Joshua Lawler, Paul Beier, Brett Dickson, Joseph Fargione, John Novembre, and David Theobald. A tribute to a true conservation innovator, Brad McRae, 1966–2017. *Conservation Biology*, 0(ja), 2018. doi: 10.1111/cobi.13235. URL https://onlinelibrary.wiley.com/doi/abs/10.1111/cobi.13235.

Thomas Lenormand. Gene flow and the limits to natural selection. *Trends in Ecology & Evolution*, 17 (4):183 – 189, 2002. ISSN 0169-5347. doi: DOI:10.1016/S0169-5347(02)02497-7. URL http://www. sciencedirect.com/science/article/pii/S0169534702024977.

David A. Levin, Yuval Peres, and Elizabeth L. Wilmer. *Markov Chains and Mixing Times*. American Mathematical Soc., 2008. ISBN 9780821886274. URL http://pages.uoregon.edu/dlevin/MARKOV/.

Simon A. Levin, Helene C. Muller-Landau, Ran Nathan, and Jérôme Chave. The ecology and evolution of seed dispersal: a theoretical perspective. *Annu. Rev. Ecol. Evol. Syst.*, 34:575–604, 2003. URL http: //arjournals.annualreviews.org/doi/pdf/10.1146/annurev.ecolsys.34.011802.132428.

Han Li and Peter Ralph. Local PCA shows how the effect of population structure differs along the genome. *Genetics*, 211(1):289–304, 2019. ISSN 0016-6731. doi: 10.1534/genetics.118.301747. URL http://www. genetics.org/content/211/1/289.

Frederick A. Matsen and John Wakeley. Convergence to the island-model coalescent process in populations with restricted migration. *Genetics*, 172(1):701–708, 2006. doi: 10.1534/genetics.105.047597. URL http: //www.genetics.org/cgi/content/abstract/172/1/701.

Henry P. McKean and Isadore M. Singer. Curvature and the eigenvalues of the Laplacian. *Journal of Differential Geometry*, 1(1-2):43–69, 1967. doi: 10.4310/jdg/1214427880. URL https://doi.org/10. 4310%2Fjdg%2F1214427880.

Brad H McRae. Isolation by resistance. *Evolution*, 60(8):1551–1561, August 2006. URL `http://www.ncbi.nlm.nih.gov/pubmed/17017056`.

Brad H McRae and Paul Beier. Circuit theory predicts gene flow in plant and animal populations. *Proc Natl Acad Sci U S A*, 104(50):19885–19890, December 2007. doi: 10.1073/pnas.0706568104. URL `https://www.ncbi.nlm.nih.gov/pmc/articles/PMC2148392/`.

Brad H. McRae, Brett G. Dickson, Timothy H. Keitt, and Viral B. Shah. Using circuit theory to model connectivity in ecology, evolution, and conservation. *Ecology*, 89(10):2712–2724, 2008. ISSN 1939-9170. doi: 10.1890/07-1861.1. URL `http://dx.doi.org/10.1890/07-1861.1`.

AJ Moreno Geraldes, N Farzaneh, CJ Grassa, AD McKown, RD Guy, SD Mansfied, CJ Douglas, and QCB Cronk. Data from: Landscape genomics of Populus trichocarpa: the role of hybridization, limited gene flow and natural selection in shaping patterns of population structure, 2014a. URL `https://doi.org/10.5061/dryad.7s848`.

Armando Moreno Geraldes, Nima Farzaneh, Christopher J. Grassa, Athena D. McKown, Robert D. Guy, Shawn D. Mansfield, Carl J. Douglas, and Quentin C. B. Cronk. Landscape genomics of *Populus trichocarpa*: the role of hybridization, limited gene flow, and natural selection in shaping patterns of population structure. *Evolution*, 68(11):3260–3280, 2014b. doi: 10.1111/evo.12497. URL `https://onlinelibrary.wiley.com/doi/abs/10.1111/evo.12497`.

M B Morrissey and D T de Kerckhove. The maintenance of genetic variation due to asymmetric gene flow in dendritic metapopulations. *Am Nat*, 174(6):875–889, December 2009. doi: 10.1086/648311. URL `https://www-journals-uchicago-edu.libproxy1.usc.edu/doi/full/10.1086/648311`.

Simon Myers, Charles Fefferman, and Nick Patterson. Can one learn history from the allelic spectrum? *Theor Popul Biol*, 73(3):342–348, May 2008. doi: 10.1016/j.tpb.2008.01.001. URL `https://www.ncbi.nlm.nih.gov/pubmed/18321552`.

Thomas Nagylaki. The expected number of heterozygous sites in a subdivided population. *Genetics*, 149 (3):1599–1604, 1998. ISSN 0016-6731. URL `http://www.genetics.org/content/149/3/1599`.

C. St J. A. Nash-Williams. Random walk and electric currents in networks. *Mathematical Proceedings of the Cambridge Philosophical Society*, 55(02):181–194, 4 1959. ISSN 1469-8064. doi: 10.1017/S0305004100033879. URL `http://journals.cambridge.org/article_S0305004100033879`.

Joseph E. Neigel, Martin R. Ball, Jr., and John C. Avise. Estimation of single generation migration distances from geographic variation in animal mitochondrial DNA. *Evolution*, 45(2):pp. 423–432, 1991. URL `http://www.jstor.org/stable/2409675`.

Pier Francesco Palamara and Itsik Pe'er. Inference of historical migration rates via haplotype sharing. *Bioinformatics*, 29(13):180–188, 2013. URL `https://www.ncbi.nlm.nih.gov/pubmed/23812983`.

Desislava Petkova, John Novembre, and Matthew Stephens. Visualizing spatial population structure with estimated effective migration surfaces. *Nat Genet*, 48(1):94–100, January 2016. doi: 10.1038/ng.3464. URL `https://www.ncbi.nlm.nih.gov/pubmed/26642242`.

R Core Team. *R: A Language and Environment for Statistical Computing*. R Foundation for Statistical Computing, Vienna, Austria, 2018. URL `https://www.R-project.org/`.

Peter Ralph and Graham Coop. The geography of recent genetic ancestry across Europe. *PLoS Biol*, 11(5): e1001555, 05 2013. doi: 10.1371/journal.pbio.1001555. URL `http://dx.doi.org/10.1371%2Fjournal.pbio.1001555`.

Peter L. Ralph. An empirical approach to demographic inference with genomic data, 2015. URL `http://arxiv.org/abs/1505.05816`. cite arxiv:1505.05816.

H Ringbauer, A Kolesnikov, D L Field, and N H Barton. Estimating barriers to gene flow from distorted isolation-by-distance patterns. *Genetics*, 208(3):1231–1245, March 2018. doi: 10.1534/genetics.117.300638. URL https://www.ncbi.nlm.nih.gov/pubmed/29311149.

Harald Ringbauer, Graham Coop, and Nicholas H Barton. Inferring recent demography from isolation by distance of long shared sequence blocks. *Genetics*, 205(3):1335–1351, March 2017. doi: 10.1534/genetics.116.196220. URL https://www.ncbi.nlm.nih.gov/pubmed/28108588.

F Rousset. Genetic differentiation and estimation of gene flow from f-statistics under isolation by distance. *Genetics*, 145(4):1219–1228, April 1997. URL http://www.ncbi.nlm.nih.gov/pubmed/9093870.

H. Bradley Shaffer, Evan McCartney-Melstad, Peter L. Ralph, Gideon Bradburd, Erik Lundgren, Jannet Vu, Bridgette Hagerty, Fran Sandmeier, Chava Weitzman, and C. Richard Tracy. Desert tortoises in the genomic age: Population genetics and the landscape. *bioRxiv*, 2017. doi: 10.1101/195743. URL https://www.biorxiv.org/content/early/2017/09/29/195743.

M Slatkin. Inbreeding coefficients and coalescence times. *Genet Res*, 58(2):167–175, October 1991. URL http://www.ncbi.nlm.nih.gov/pubmed/1765264.

Curtis Strobeck. Average number of nucleotide differences in a sample from a single subpopulation: a test for population subdivision. *Genetics*, 117(1):149–153, September 1987. URL http://www.ncbi.nlm.nih.gov/pubmed/17246396.

D.W. Stroock and S.R.S. Varadhan. *Multidimensional Diffusion Processes*. Grundlehren der mathematischen Wissenschaften. Springer Berlin Heidelberg, 1997. ISBN 9783540903536.

L Sundqvist, K Keenan, M Zackrisson, P Prodöhl, and D Kleinhans. Directional genetic differentiation and relative migration. *Ecol Evol*, 6(11):3461–3475, 06 2016. doi: 10.1002/ece3.2096. URL https://www.ncbi.nlm.nih.gov/pubmed/27127613.

Jonathan Terhorst and Yun S Song. Fundamental limits on the accuracy of demographic inference based on the sample frequency spectrum. *Proc Natl Acad Sci U S A*, 112(25):7677–7682, June 2015. doi: 10.1073/pnas.1503717112. URL https://www.ncbi.nlm.nih.gov/pubmed/26056264.

John Wakeley. *Coalescent Theory, an Introduction*. Roberts and Company, Greenwood Village, CO, 2005. URL http://www.coalescenttheory.com/.

John Wakeley, Léandra King, Bobbi S Low, and Sohini Ramachandran. Gene genealogies within a fixed pedigree, and the robustness of Kingman's coalescent. *Genetics*, 190(4):1433–1445, April 2012. doi: 10.1534/genetics.111.135574. URL http://www.ncbi.nlm.nih.gov/pubmed/22234858.

Ian J. Wang and Gideon S. Bradburd. Isolation by environment. *Molecular Ecology*, 23(23):5649–5662, 2014. ISSN 1365-294X. doi: 10.1111/mec.12938. URL http://dx.doi.org/10.1111/mec.12938.

Robin S. Waples and James R. Faulkner. Modelling evolutionary processes in small populations: not as ideal as you think. *Molecular Ecology*, 18(9):1834–1847, 2009. doi: 10.1111/j.1365-294X.2009.04157.x. URL https://onlinelibrary.wiley.com/doi/abs/10.1111/j.1365-294X.2009.04157.x.

Michael C Whitlock and Nicholas H Barton. The effective size of a subdivided population. *Genetics*, 146 (1):427–441, May 1997. URL http://www.ncbi.nlm.nih.gov/pubmed/9136031.

Jon F. Wilkins. A Separation-of-Timescales Approach to the Coalescent in a Continuous Population. *Genetics*, 168(4):2227–2244, 2004. doi: 10.1534/genetics.103.022830. URL http://www.genetics.org/cgi/content/abstract/168/4/2227.

Gregory A. Wilson and Bruce Rannala. Bayesian inference of recent migration rates using multilocus genotypes. *Genetics*, 163(3):1177–1191, 2003. URL http://www.genetics.org/content/163/3/1177.long.

Kimberly A. With. The landscape ecology of invasive spread. *Conservation Biology*, 16(5):1192–1203, 2002. ISSN 1523-1739. doi: 10.1046/j.1523-1739.2002.01064.x. URL `http://dx.doi.org/10.1046/j.1523-1739.2002.01064.x`.

# A    The simplest example

To demonstrate the main theoretical ideas, we provide a short example. Consider a Markov chain with two states, where the rate of movement from state 1 to state 2 is $G_{12}$ and the rate of movement from state 2 to state 1 is $G_{21}$, so the generator matrix is

$$G = \begin{bmatrix} -G_{12} & G_{12} \\ G_{21} & -G_{21} \end{bmatrix}.$$

Equation 7 equates two $2 \times 2$ matrices, so provides four equations. Only three of these are unique; simplifying these and using that $C_{12} = C_{21}$, these are:

$$2\left(C_{12} - C_{11}\right) G_{12} - C_{11}\gamma_1 = -1$$
$$\left(C_{11} - C_{12}\right) G_{21} + \left(C_{22} - C_{12}\right) G_{12} = -1$$
$$2\left(C_{12} - C_{22}\right) G_{21} - C_{22}\gamma_2 = -1.$$

Given $C$, we have three equations for the four unknowns, $G_{12}$, $G_{21}$, $\gamma_1$, and $\gamma_2$, which we can solve symbolically. The valid solutions to these equations are those with $G_{12}$, $G_{21}$, $\gamma_1$, and $\gamma_2$ nonnegative. If $C_{11} \neq C_{12}$, we can write the solution with $\gamma_1$ as the free variable:

$$G_{12} = \frac{1}{2(C_{11} - C_{12})} - \frac{C_{11}}{2(C_{11} - C_{12})}\gamma_1$$
$$G_{21} = \frac{-2(C_{11} - C_{12}) + (C_{12} - C_{22})}{2(C_{11} - C_{12})^2} - \frac{C_{11}(C_{12} - C_{22})}{2(C_{11} - C_{12})^2}\gamma_1$$
$$\gamma_2 = \frac{(C_{11} - 2C_{12} + C_{22})^2}{C_{22}(C_{11} - C_{12})^2} - \frac{C_{11}(C_{12} - C_{22})^2}{C_{22}(C_{11} - C_{12})^2}\gamma_1.$$

This implies that $\gamma_2$ decreases as $\gamma_1$ increases as long as $C_{12} \neq C_{22}$. This makes sense because increasing a rate of coalescence cannot make expected coalescence times longer, so in order to keep coalescence times the same, if one coalescence rate is increased, another must be decreased. This also implies that, in order for $\gamma_2$ to be a value other than 0, we must have $C_{11} - 2C_{12} + C_{22} \neq 0$. In general, if there is a value or range of values of $\gamma_1$ for which the other movement and coalescence parameters are non-negative, then a solution exists.

To produce a concrete example, suppose that $C_{11} = 1$, $C_{12} = 2$, and $C_{22} = 1.5$ in arbitrary time units. The other parameters will be non-negative when $1 \leq \gamma_1 \leq 5$, as shown in in Figure S1. Assuming $\gamma_1 = \gamma_2$ produces a unique solution, with $\gamma_1 = \gamma_2 = 1.29$ and $G_{12} = 0.14$ and $G_{21} = 0.93$.

# B    Finding $G$ from $H$

Suppose that $G$ is the generator matrix of an irreducible continuous-time Markov chain $X$ on at least two states, so that $G_{ij} \geq 0$ for $i \neq j$ and $G\mathbf{1} = 0$. Under these assumptions, there is a unique stationary distribution, $\pi$, that satisfies $\pi^T \mathbf{1} = 1$ and $\pi^T G = 0$. Let $\tau_j = \inf\{t \geq 0 : X_t = j\}$ and $H_{ij} = \mathbb{E}[\tau_j \mid X_0 = i]$. Then we know that

$$(GH)_{ij} = -1 \qquad \text{for } i \neq j,$$

and hence that for some vector $x$,

$$GH = -\mathbf{1}\mathbf{1}^T + \operatorname{diag}(x). \tag{9}$$

What is $x$? First note that the Random Target Lemma [Aldous and Fill, 2002] tells us that if $\pi$ is the stationary distribution of the chain, then $(H\pi)_i$ does not depend on $i$, and so there exists a vector $\nu \propto \pi$ such that $H\nu = \mathbf{1}$. Multiplying equation (9) by $\nu$, we get that

$$0 = G\mathbf{1} = (\operatorname{diag}(x) - \mathbf{1}\mathbf{1}^T)\nu,$$
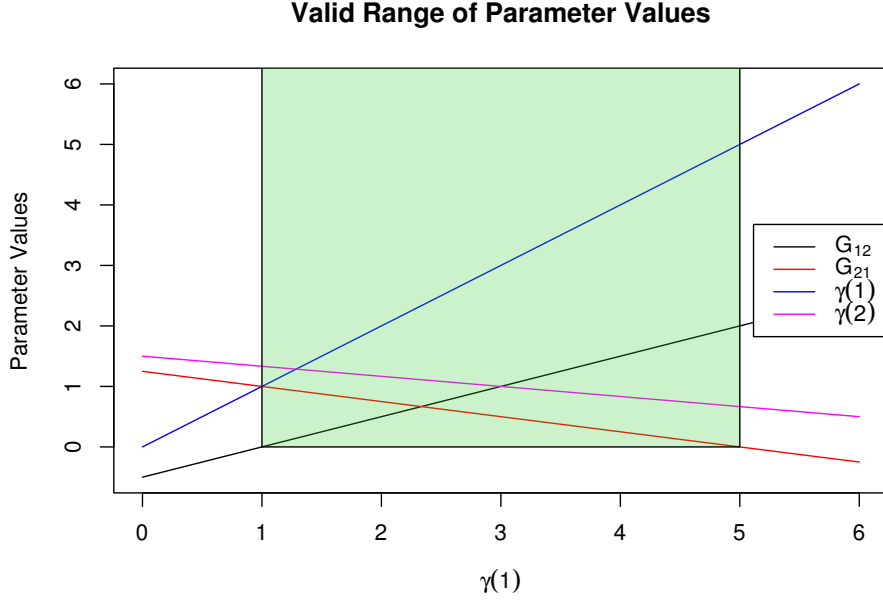
**Valid Range of Parameter Values**



Figure S1: The green shaded region shows the valid range of the parameter values for the two state Markov chain given that $C_{11} = 1$, $C_{12} = 2$, and $C_{22} = 1.5$

which rearranges to

$$x_i = \frac{\mathbf{1}^T \nu}{\nu_i}.$$

But, since $\nu \propto \pi$, it must be that $\pi = \nu/\mathbf{1}^T \nu$, and so $x_i = 1/\pi_i$.

Now, we prove that $H$ is in fact invertible, by showing that $z^T H \neq 0$ for every nonzero vector $z$. First note that $\mathbf{1}^T H \neq 0$, since the entries of $H$ are nonnegative. Now take $z$ orthogonal to $\mathbf{1}$. Since the chain is irreducible, the eigenspace associated with the eigenvalue 0 for $G$ has multiplicity one, and so any vector $y$ that satisfies $y^T G = 0$ is proportional to $\pi$. This implies that there is a vector $y$ such that $y^T G = z^T$. Multiplying equation (9) on the left by $y^T$ obtains $z^T H = y^T (\mathrm{diag}(1/\pi) - \mathbf{11}^T)$. If $H$ is not invertible, then there is a $z$ for which this is zero, i.e., $y_i/\pi_i = \sum_j y_j$ for every $i$. But, this only holds if $y = \pi$, which was disallowed, because then we would have $z = 0$. Therefore, $H$ is invertible.

In summary, $\pi = H^{-1}\mathbf{1}/\mathbf{1}^T H^{-1}\mathbf{1}$, and

$$G = (\mathrm{diag}(1/\pi) - \mathbf{11}^T)H^{-1}. \tag{10}$$

Note that this equation only specifies $H$ up to a constant added to each column: i.e., if given $G$ one obtains a matrix $Y$ solving $GY = \mathrm{diag}(1/\pi) - \mathbf{11}^T$, then $H_{ij} = Y_{ij} - Y_{jj}$.

# C  Equality of commute and coalescence times

Under what conditions are coalescence times and commute times (with some local diversity values) equal? In other words, for what choices of $G$, $\gamma$, and $q$ does

$$\widetilde{R} = (H + H^T)/4 + (q\mathbf{1}^T + \mathbf{1}q^T)/2 \tag{11}$$

29

888 solve equation (7)? Writing this out, this says that

$$(GH + (GH)^T + GH^T + (GH^T)^T)/4 + (Gq\mathbf{1}^T + \mathbf{1}(Gq)^T)/2 = \mathrm{diag}(q)\,\mathrm{diag}(\gamma) - \mathbf{1}\mathbf{1}^T. \tag{12}$$

889 (To simplify this we used the fact that $\mathrm{diag}(H) = 0$ and $G\mathbf{1} = 0$.)

890     It is not clear what can be said about the general case because of the presence of $HG^T$, but if we assume
891 that $H$ is symmetric, we can make progress, because then we have that $GH = GH^T$, and so equation (9)
892 says that all four terms in the first group are equal, and equation (12) simplifies to

$$\mathrm{diag}(1/\pi) + (Gq\mathbf{1}^T + \mathbf{1}(Gq)^T)/2 = \mathrm{diag}(q)\,\mathrm{diag}(\gamma), \tag{13}$$

893 where the $-\mathbf{1}\mathbf{1}^T$ terms on each side canceled. Because $G\mathbf{1} = 0$, the most obvious solution to this is if $q = c\mathbf{1}$
894 and $c\gamma = 1/\pi$, for some constant $c$ (although there is a broader family of solutions).

895     In summary, if hitting times are symmetric and coalescence rates are equal to the inverse of the stationary
896 distribution, then coalescence times are equal to commute times plus one. This is fairly restrictive, but does
897 occur if the population configuration is isotropic (as for instance in an all-connected-to-all island model with
898 equal migration rates) or in populations arranged around a ring with migration rates depending only on the
899 distance between them.

900     Can we solve equation (13) more generally? For that equation to hold, we need $Gq\mathbf{1}^T + \mathbf{1}(Gq)^T$ to be
901 diagonal, i.e., that $(Gq)_i + (Gq)_j = 0$ for all $i \neq j$. For any $k \neq \ell$, there exists a vector $u^{(k\ell)}$ such that
902 $(Gu^{(k\ell)})_i = \delta_{ik} - \delta_{i\ell}$; the only possible $q$ for which $Gq\mathbf{1}^T + \mathbf{1}(Gq)^T$ is diagonal are of the form $q = \alpha\mathbf{1} + \beta u^{(k,\ell)}$
903 for some $k \neq \ell$ and some constants $\alpha$ and $\beta$. We would then need

$$1/\pi_i + \delta_{ik} - \delta_{i\ell} = q_i\gamma_i \qquad \text{for all} \quad i. \tag{14}$$

904 This implies that for any Markov chain with symmetric hitting times, we can find diversity values ($q$) and
905 coalescence rates ($\gamma$) that make $\widetilde{R} = C$ (and in fact there are many ways to do this). However, there is not
906 a general solution for $q$ if coalescence rates are also given (as is the case in practice). This is related to the
907 fact proved by Strobeck [1987] (and generalized by Nagylaki [1998]) that $\mathrm{diag}(C)$ is constant and does not
908 depend on movement rates for any isotropic conservative migration model.
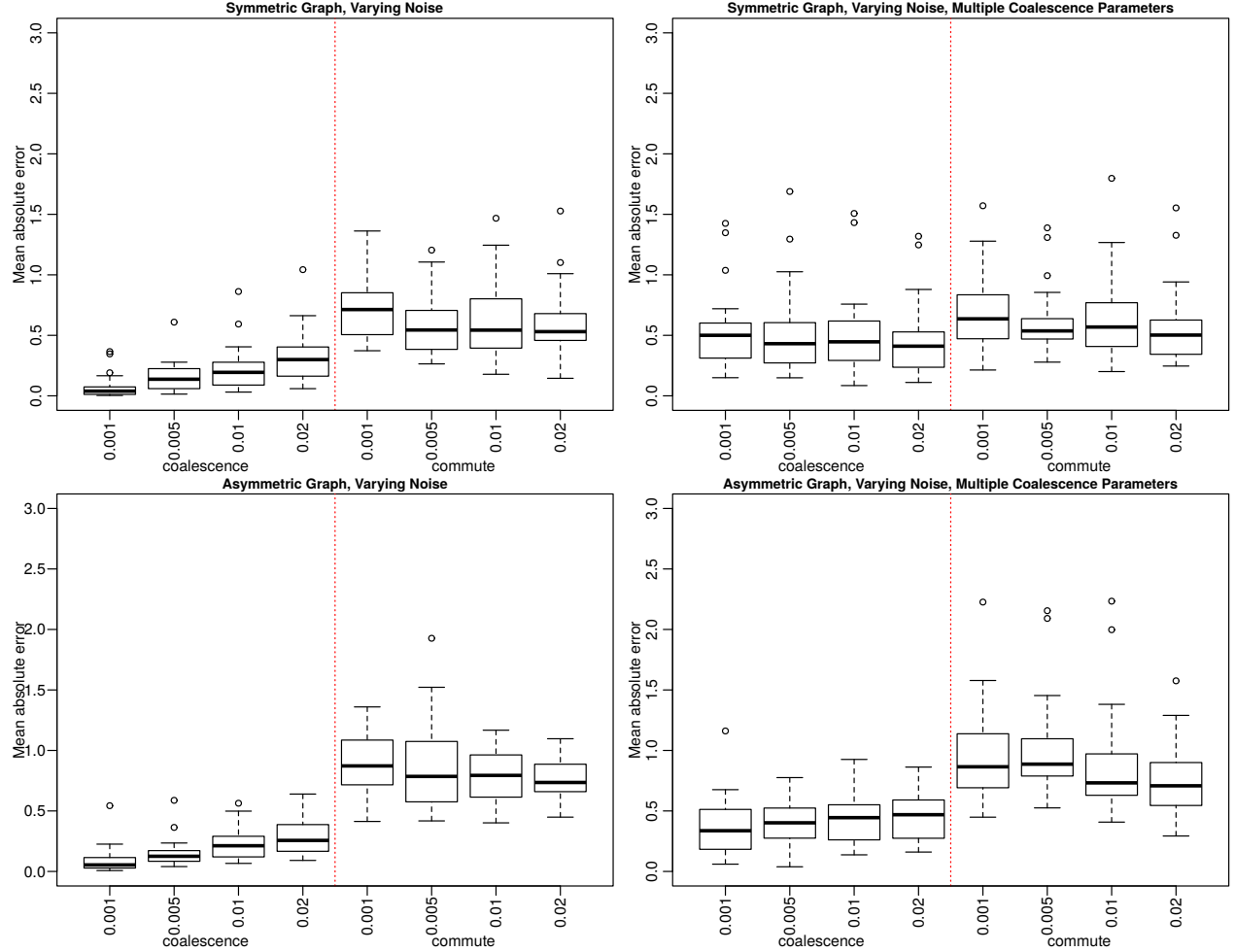
30

Figure S2: Boxplots of the mean absolute error defined to be the absolute value difference between the true value and posterior median, averaged across movement parameters $g$ for each of the 25 graphs in each situation. Each box is labeled with the relative amount of noise added to $C$ to produce the values used for inference. The top left shows the results for symmetric graphs when there is a single coalescence parameter for all locations, the top right for symmetric graphs when there is a separate coalescence parameter for each location, the bottom left for asymmetric graphs when there is a single coalescence parameter for all locations, and the bottom right for asymmetric graphs when there is a separate coalescence parameter for each location.
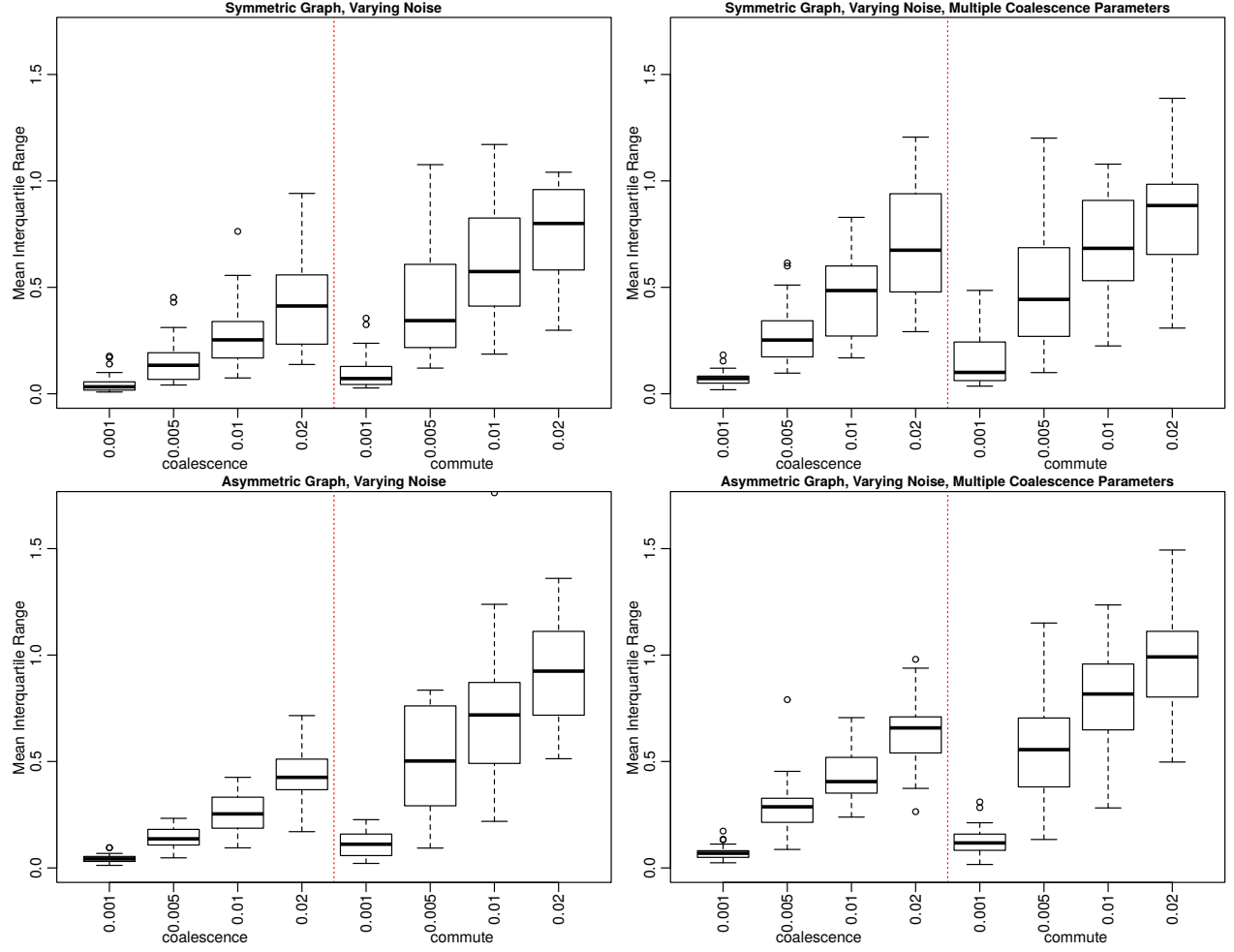
Figure S3: Boxplots of the mean interquartile ranges of the posterior distributions of $g$ for each of the 25 graphs in each situation. Each box is labeled with the relative amount of noise added to $C$ to produce the values used for inference. Subplot locations for each situation are the same as in Figure S2.
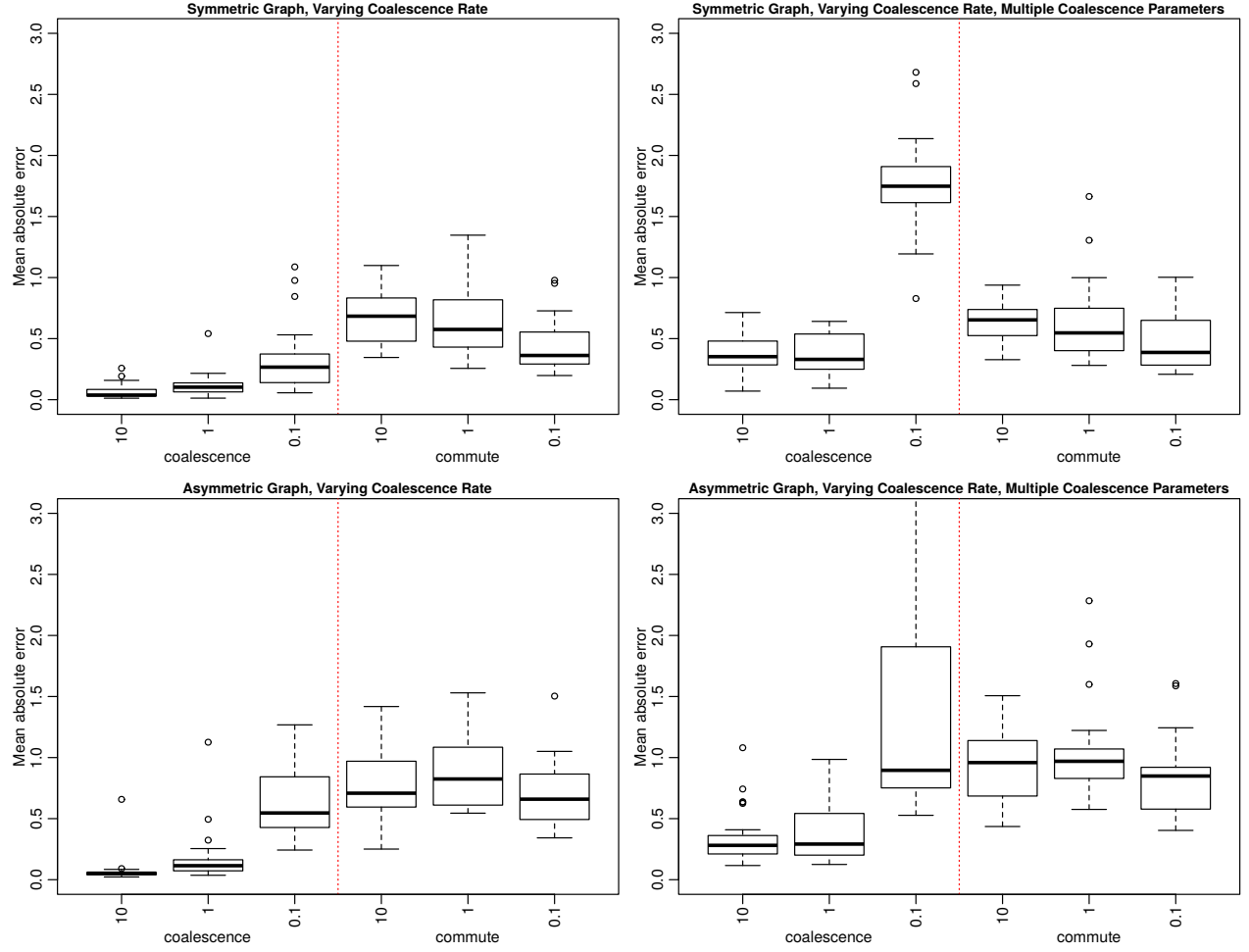
Figure S4: Boxplots of the mean absolute error, defined to be the absolute value difference between the true value and posterior median, averaged across movement parameters $g$ for each of the 25 graphs in each situation. Each box is labeled with the coalescence rate in the underlying model for each situation. Subplot locations for each situation are the same as in Figure S2.

Figure S5: Boxplots of the mean interquartile ranges of the posterior distributions of $g$ for each of the 25 graphs in each situation. Each box is labeled with the coalescence rate in the underlying model for each situation. Subplot locations for each situation are the same as in Figure S2.
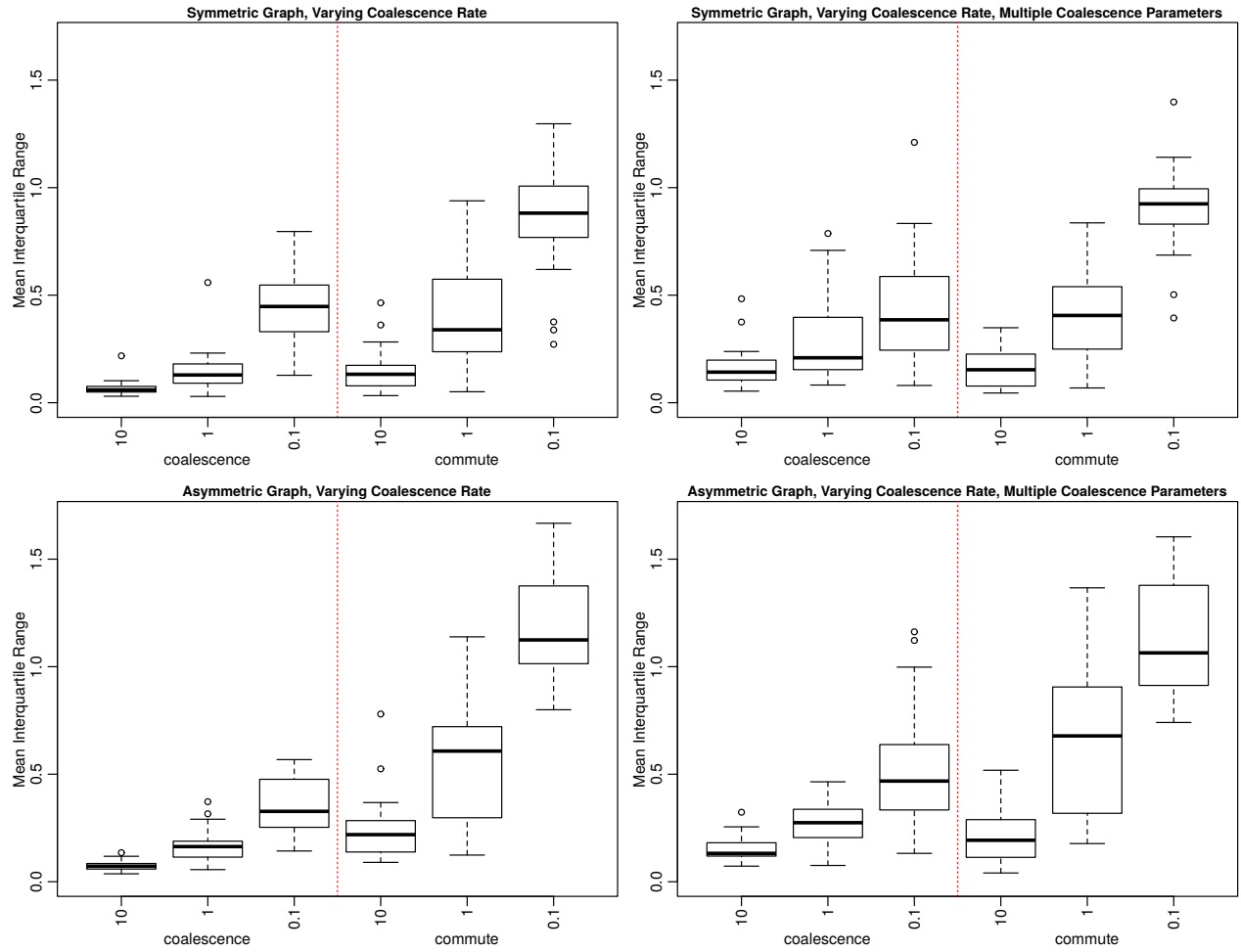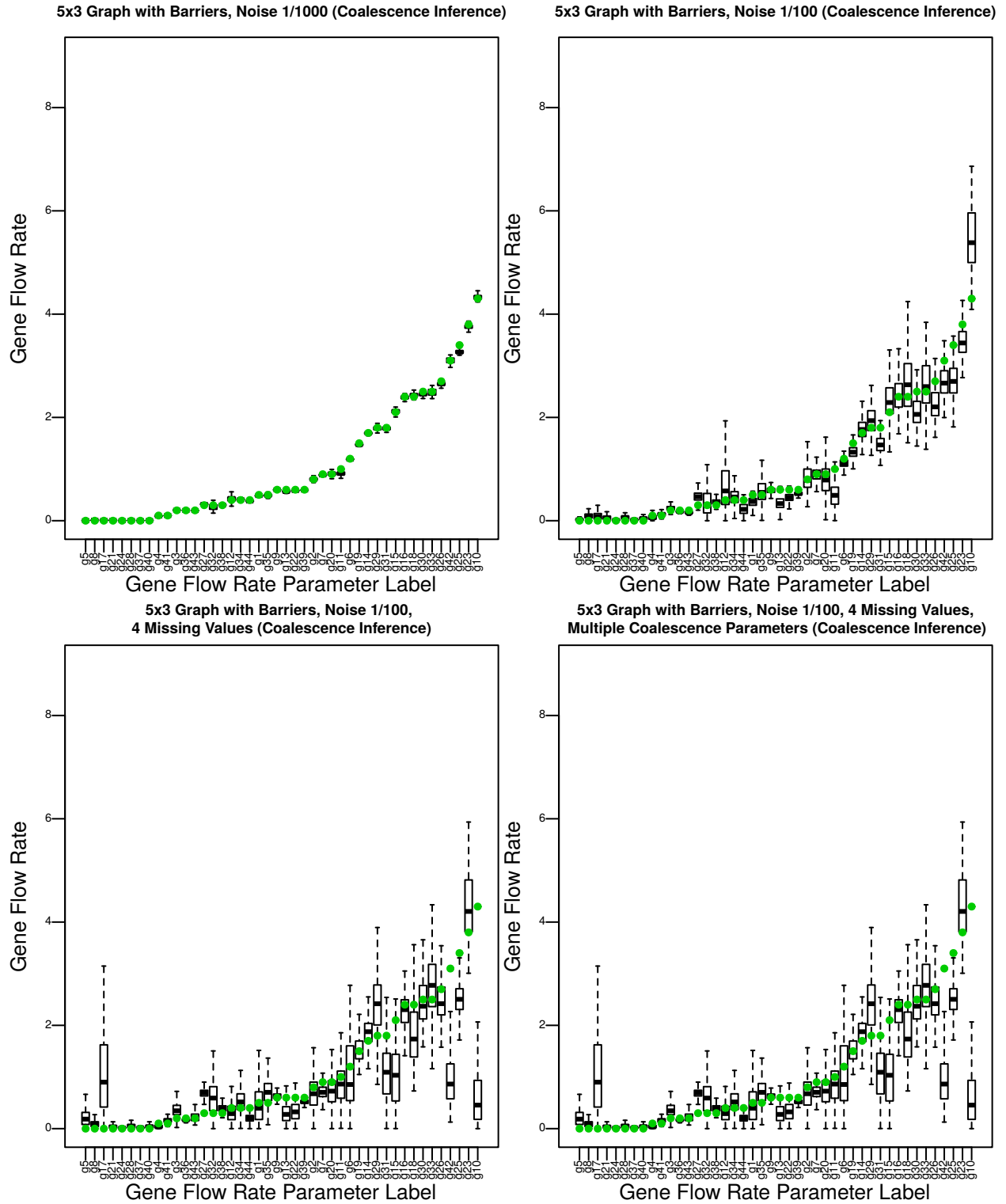
Figure S6: Posterior distributions for values of $g$ for the $5 \times 3$ graph with barriers for each of the analysis cases with coalescence time inference. See Figure 2 to see movement parameter locations.
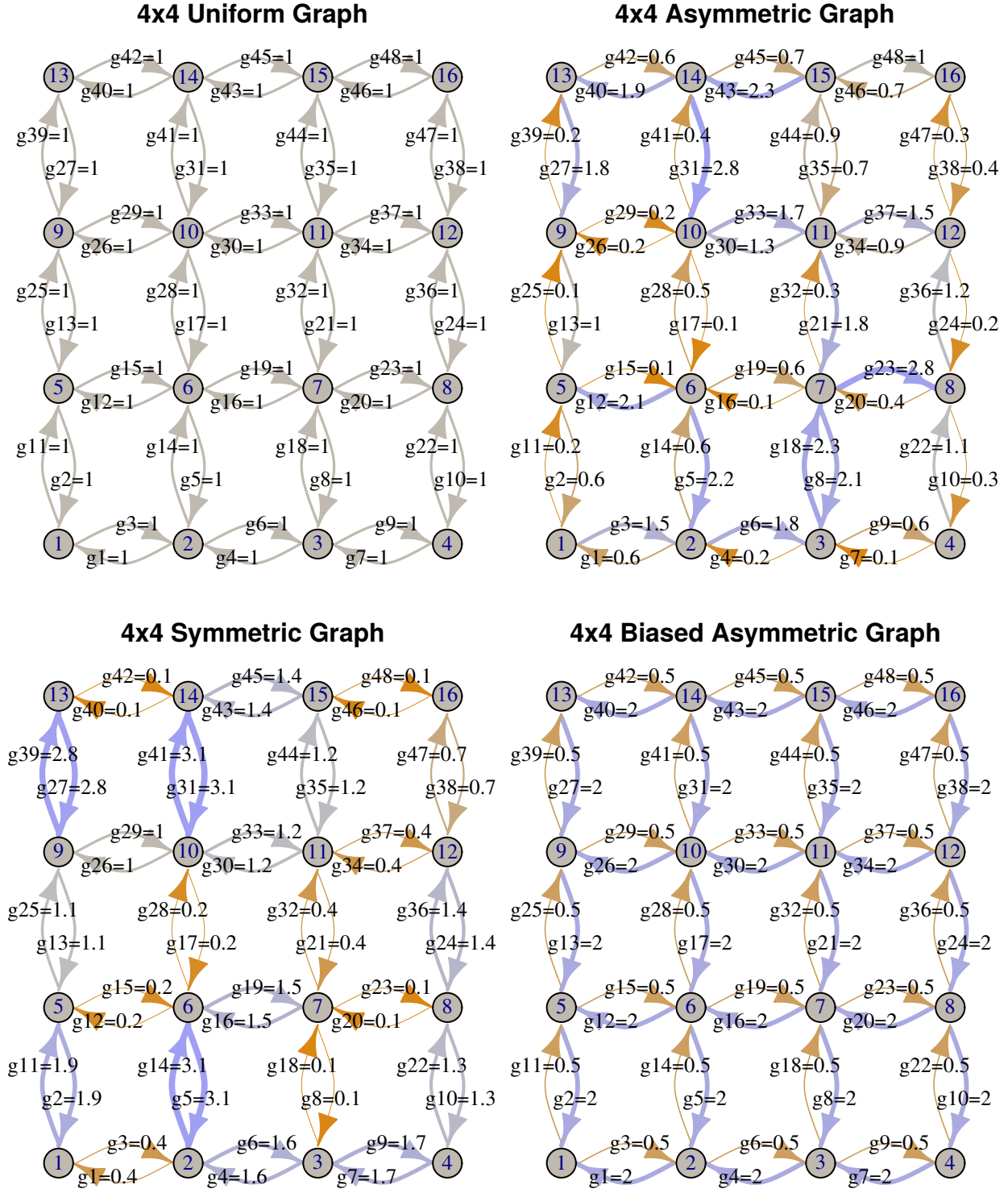
Figure S7: Grid structure and gene flow rates for the uniform graph, symmetric graph, the asymmetric graph, and the biased asymmetric graph using the igraph R package.
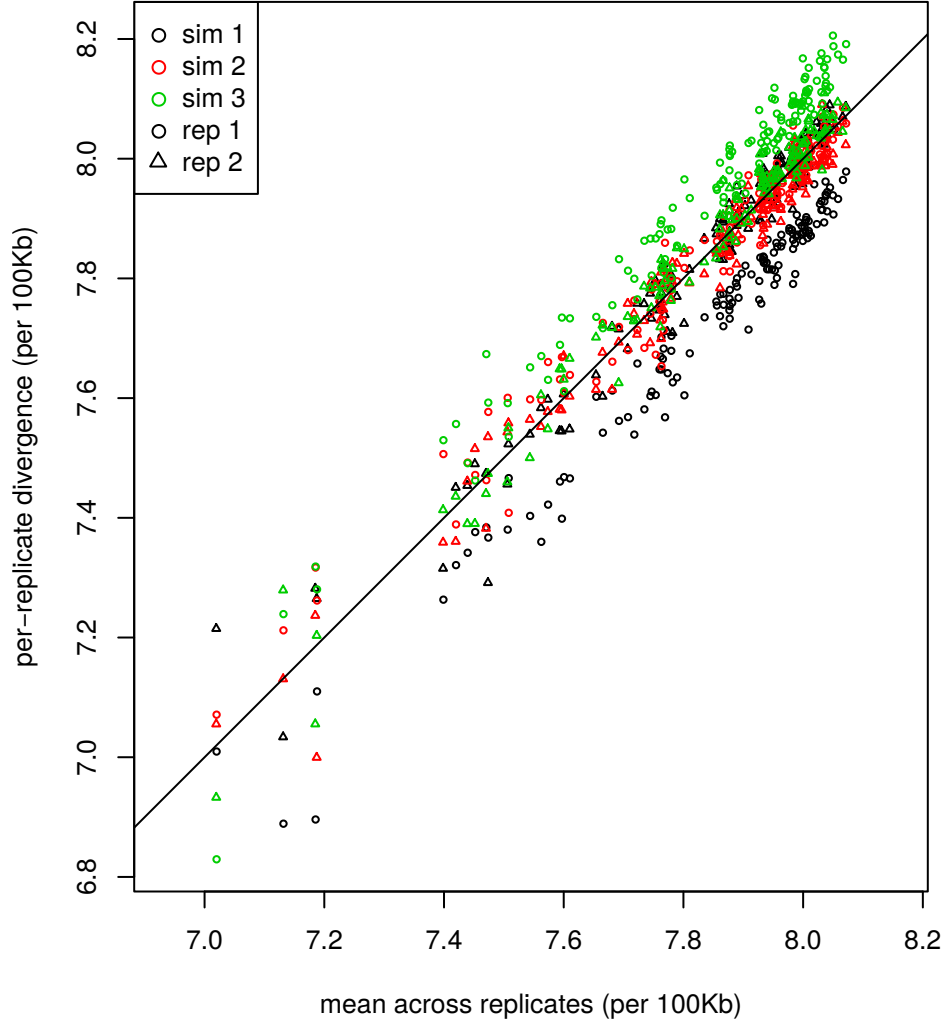
Figure S8: Comparison of mean coalescence times between samples and between replicates for a $4 \times 4$ discretization of a square landscape with uniform migration. Between the 16 geographic regions, there are 136 comparisons; these are shown for two nonoverlapping samples taken from three independent replicate simulations, each plotted against the mean value across all replicates. Colors denote simulation replicate, and point type (circle/triangle) denotes the sample. Without sampling or process noise, all points would fall on the $y = x$ line. Among the six sets of observations, simulation replicate explains 6.7% of the variance, and spatial sampling explains 13.8% of the variance.
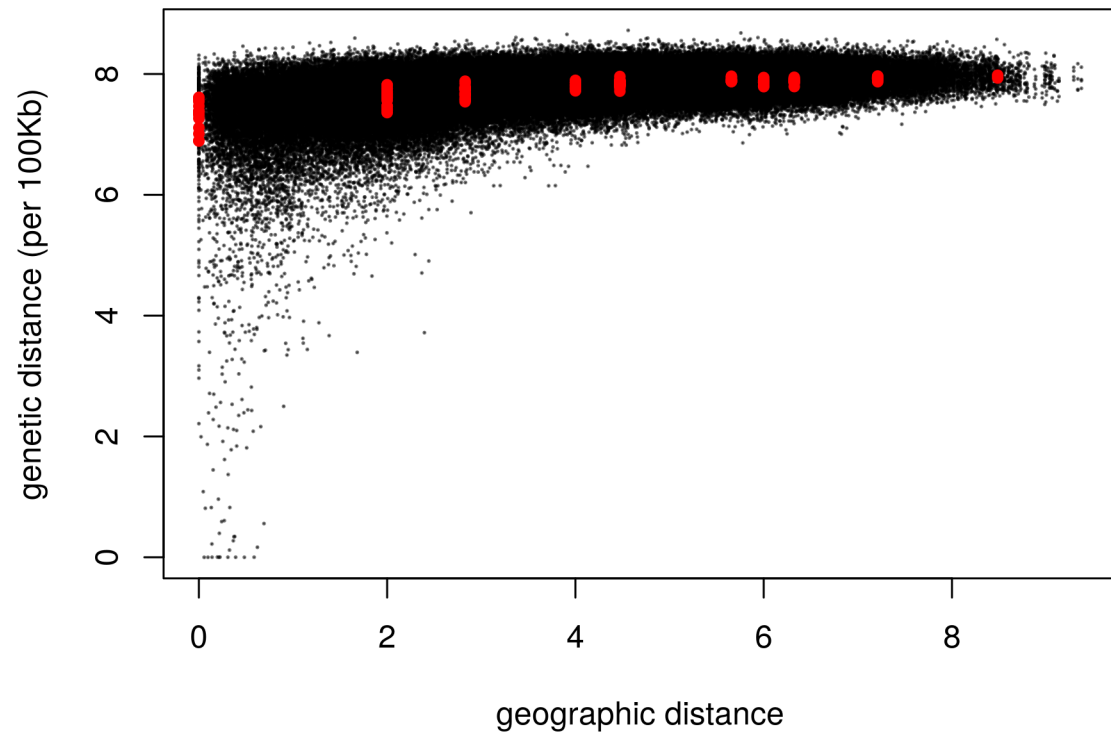
Figure S9: Genetic distance against geographic distance between all pairs of sampled individuals on a square landscape with uniform migration. Red dots denote mean genetic distances between sampled individuals from a $4 \times 4$ discretization of the landscape, as used for instance in Figure 7.
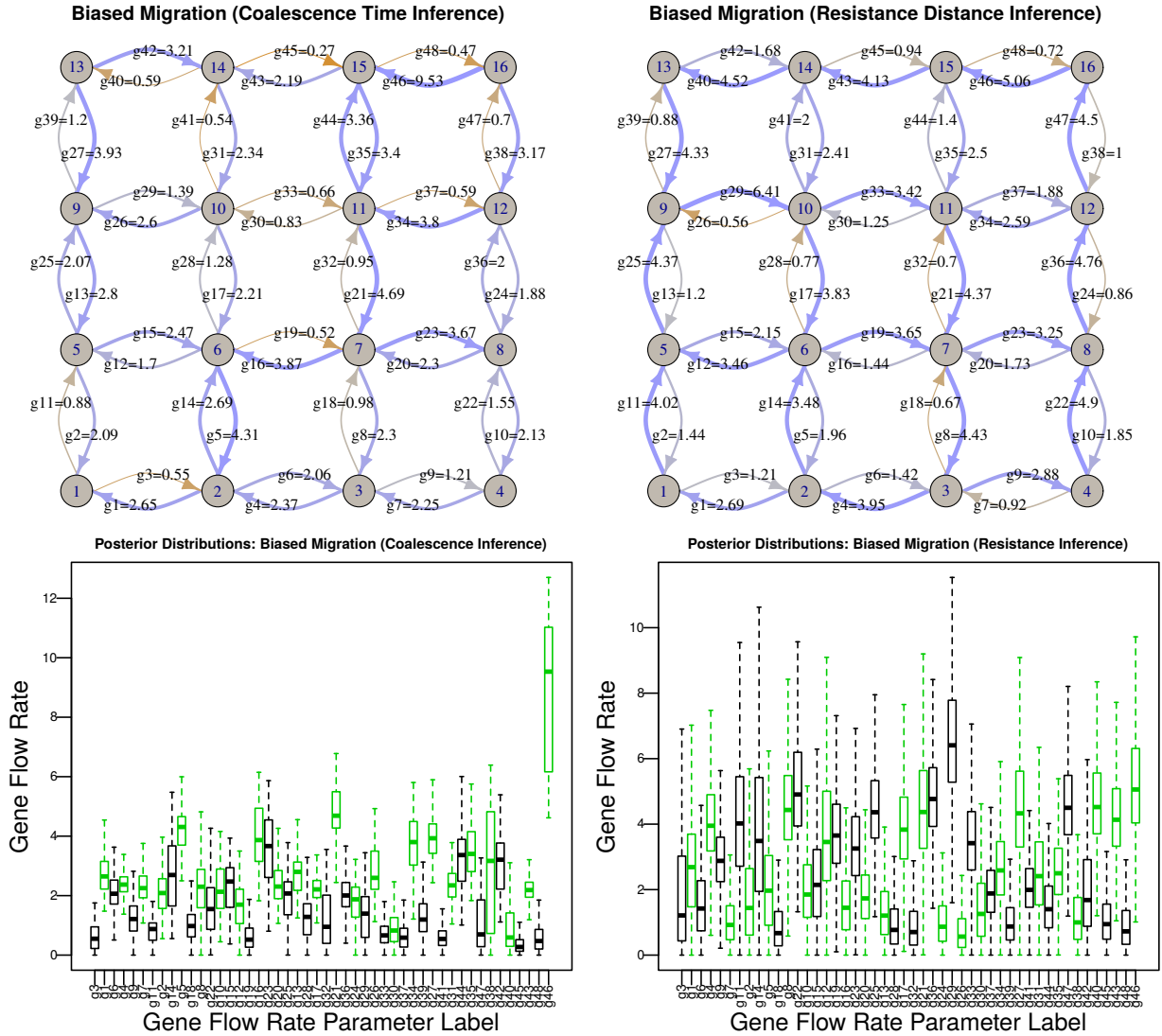
Figure S10: **(Above:)** Posterior medians and **(below)** posterior distributions of the inferred values of $g$ for the $4 \times 4$ discretization of the square landscape with biased migration, inferred with the **(left)** coalescence time-based, and **(right)** resistance distance-based method. In the boxplots, black boxes show posterior distributions of gene flow rates up and to the right, and the adjacent green box corresponds to gene flow rate along the same edge in the opposite direction.

Figure S11: Results from the **barrier** simulation: **(top left)** Positions of all individuals at the end of simulation. **(top right)** mean migration rates as estimated by EEMS. Below are shown posterior median migration rates as estimated using **(middle left)** the coalescence time method and **(middle right)** the resistance distance method. Last are shown the posterior distributions, for **(bottom left)** the coalescence time method and **(bottom right)** the resistance distance method.
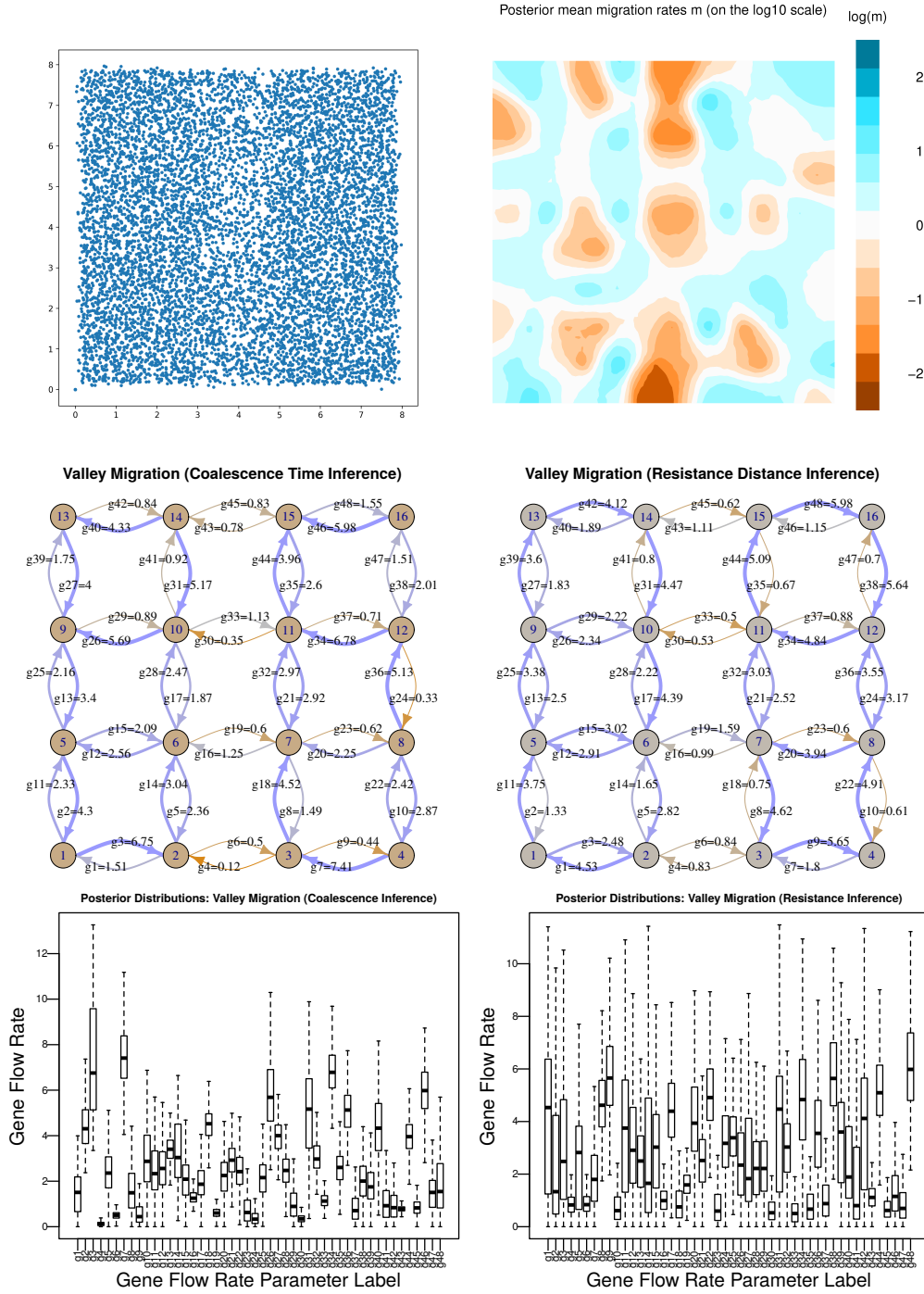
Figure S12: Results from the **valley** simulation: **(top left)** Positions of all individuals at the end of simulation. **(top right)** mean migration rates as estimated by EEMS. Below are shown posterior median migration rates as estimated using **(middle left)** the coalescence time method and **(middle right)** the resistance distance method. Last are shown the posterior distributions, for **(bottom left)** the coalescence time method and **(bottom right)** the resistance distance method.
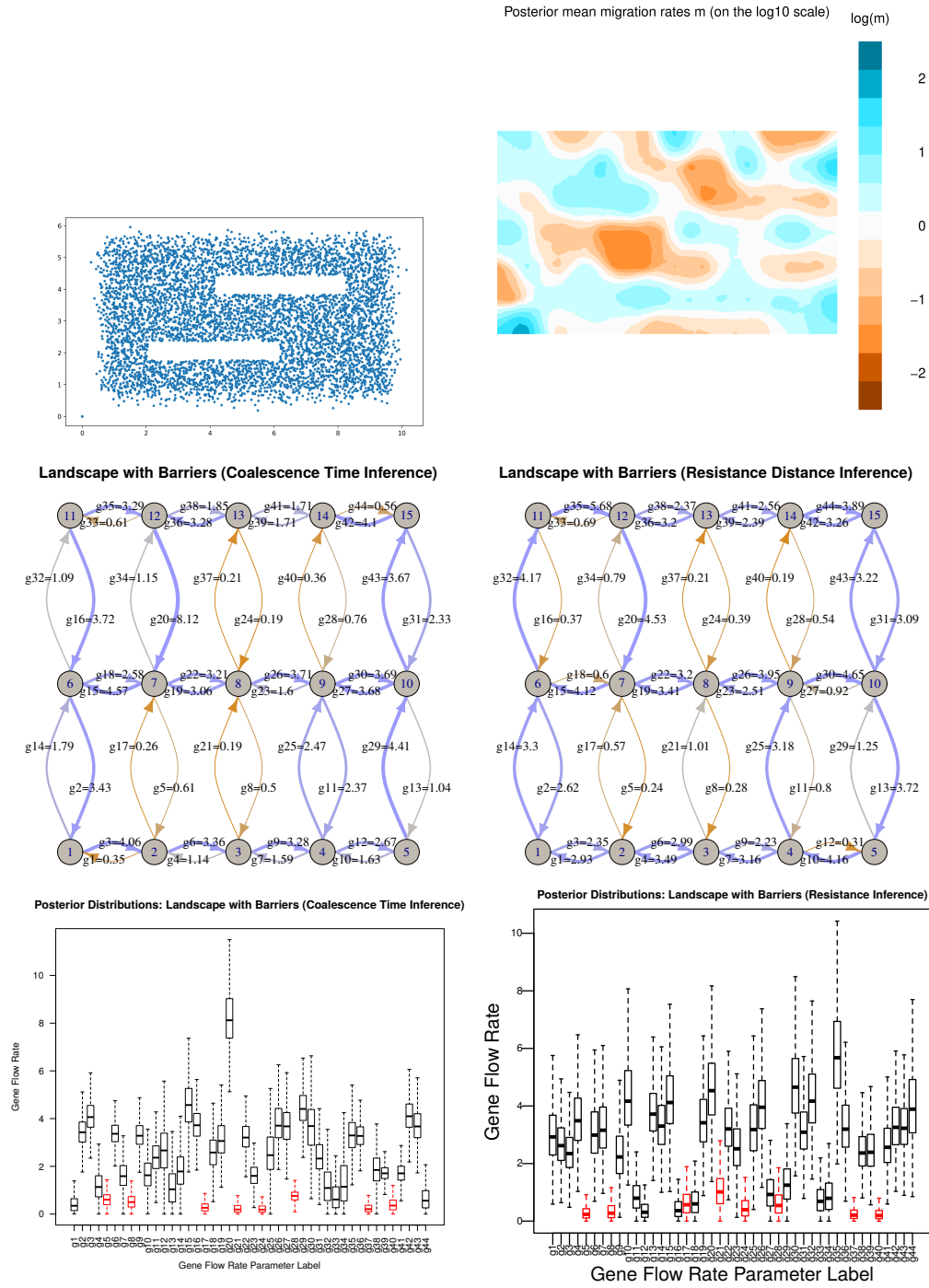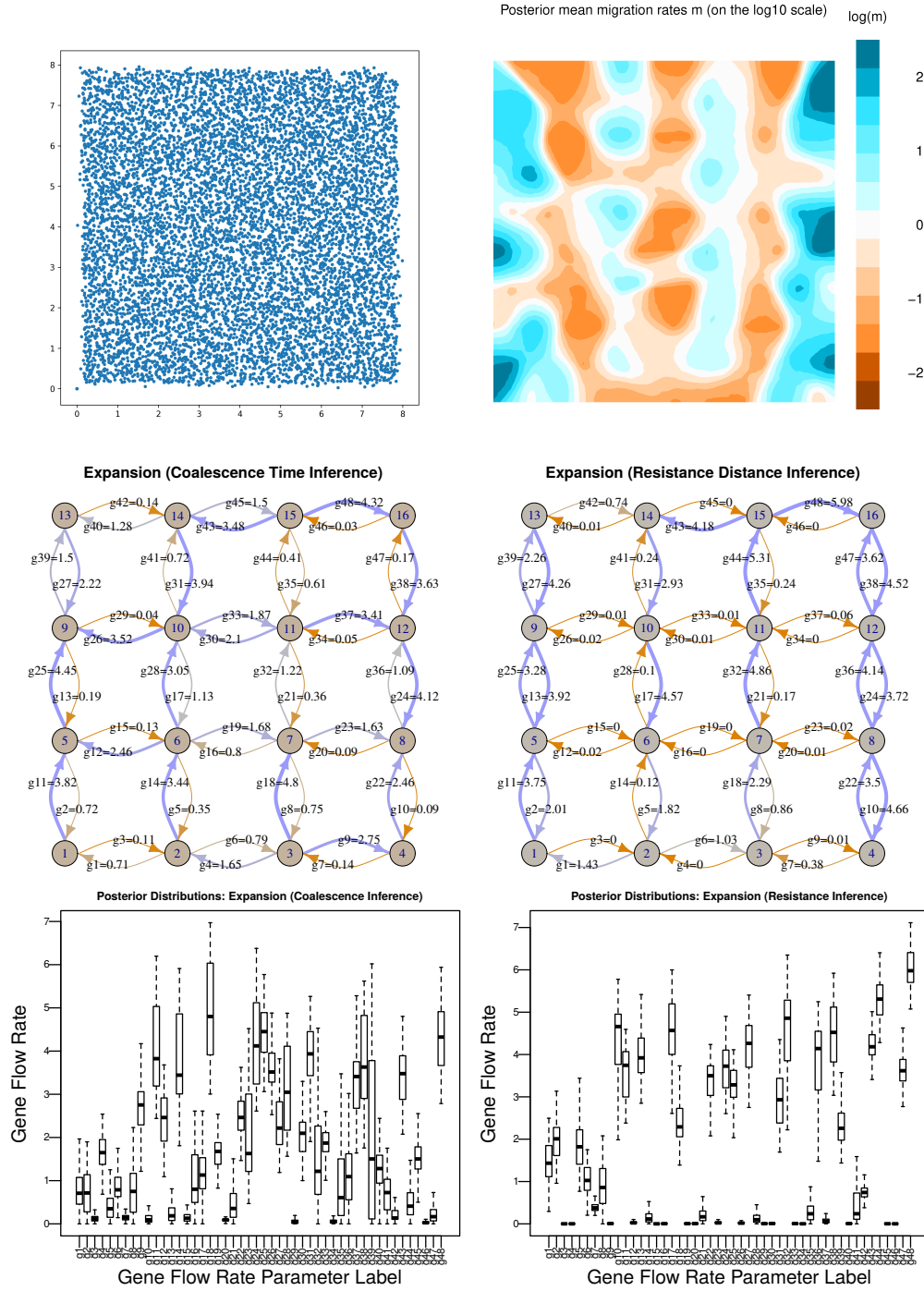
Figure S13: Results from the **expansion** simulation: **(top left)** Positions of all individuals at the end of simulation. **(top right)** mean migration rates as estimated by EEMS. Below are shown posterior median migration rates as estimated using **(middle left)** the coalescence time method and **(middle right)** the resistance distance method. Last are shown the posterior distributions, for **(bottom left)** the coalescence time method and **(bottom right)** the resistance distance method.
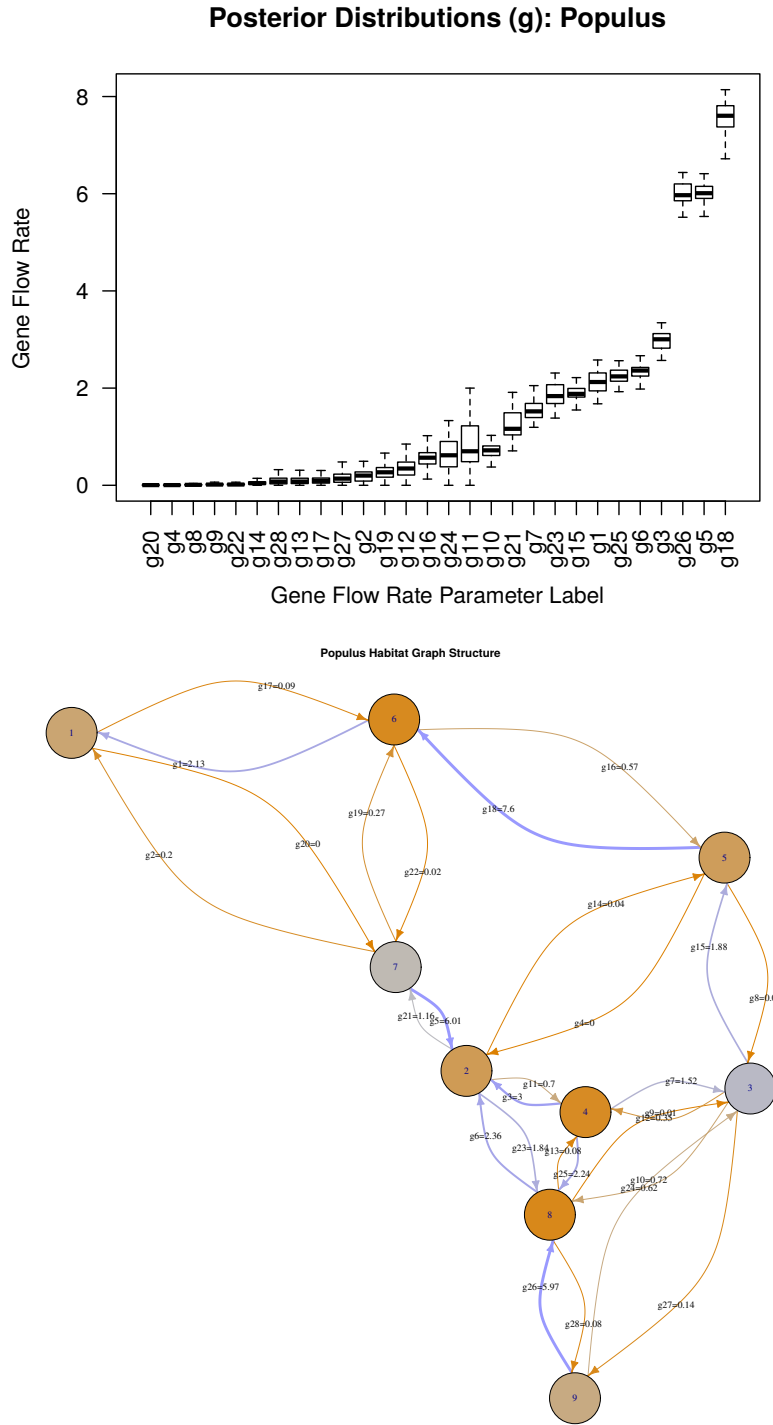
Figure S14: Posterior distributions of parameters for *Populus* data, using coalescence time inference with the model shown in Figure 8. **(top)** Posterior medians (dark line), approximate middle 50% (box), and 90% (whiskers), for gene flow rates. **(bottom)** Posterior medians gene flow rates, both as a numerical label and color (as in other figures, red is lower and blue is larger), along with edge labels that match the upper figure. Nodes are also colored according to posterior median coalescence rate: grey is a high rate (small population) and orange is a low rate (large population).

43

**Posterior Distributions (gamma): Populus**
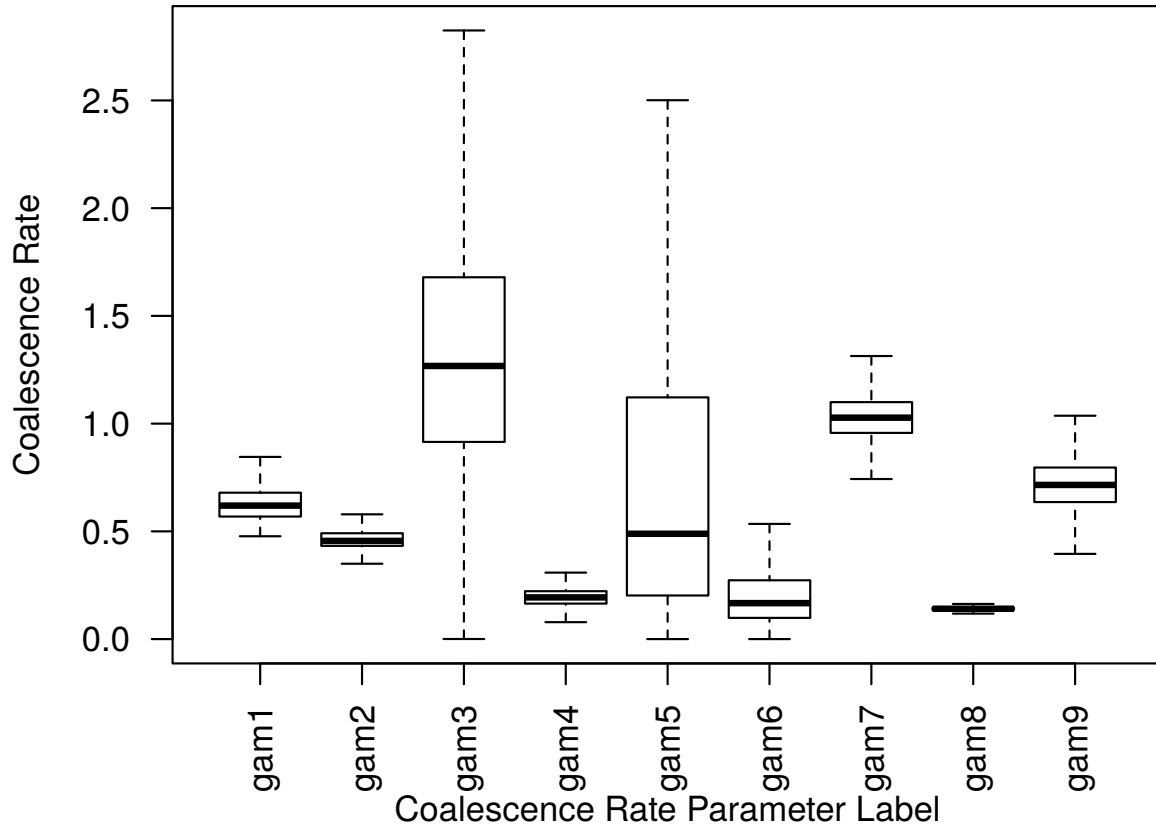
Figure S15: Posterior distributions of parameters for *Populus* data, using coalescence time inference with the model shown in Figure 8. Plot shows posterior medians (dark line), approximate middle 50% (box), and 90% (whiskers), for coalescence rates, labeled as in Figure 8. For instance, the coalescence rates for regions 4 and 8 (labeled "gam4" and "gam8") are inferred to be much smaller than most other regions, perhaps indicating larger or older populations in southwestern British Columbia.

Resubmission Cover Letter

*Molecular Ecology Resources*

Erik Lundgren

*and* Peter Ralph

April 22, 2019

**To the Editor(s) –**

We are writing to submit a revised version of our manuscript, "Are populations like a circuit? Comparing isolation by resistance to a new coalescent-based method." (formerly titled "Are populations like a circuit? The relationship between isolation by distance and isolation by resistance").

Thanks to the five mostly anonymous reviewers for their many useful comments – we've addressed all of them, which we think has made the paper more generally understandable and suitable for this audience. In particular, we have included analysis of an empirical dataset (which was fun, and produced good results), revised the figures for increased legibility, and added a substantial amount of additional explanation of the technical points. We hope that discussion of the empirical results should help make interpretation of the coalescent-based model more broadly understandable. And, at the suggestion of reviewer 1, we have changed the title. We think this has all improved the paper substantially, and hope you agree.

We have included detailed responses to all the reviewer's comments, with page and line numbers that refer to the revised version of the manuscript. We are also including a file with changes made since the first submission highlighted (named `ibc-diff.pdf`). Finally, we are including an additional pdf (named `isolation_by_coalescence.pdf`) that has the paper, the supplementary material, and the responses to reviewers all in one place in which the page/line numbers in the reviews are hyperlinks to the correct location in the main document.

**Sincerely,**

**Erik Lundgren and Peter Ralph**

# Reviewer AE:

We received five reviews for your submitted article. While three are quite positive, two others are more critical. In the balance of comments, all reviewers felt that your article should be published in MER, though significant improvements were requested. Therefore, my decision is to request a revision before accepting your article.

Please respond to all major comments raised by the reviewers. In particular, try to address the following points: 1) Revise figures for clarity and legibility. 2) Include an empirical dataset, as suggested by REV 2. 3) Rewrite for a broader audience of biologists (translating some difficult concepts when possible and as appropriate). 4) Clarify aspects of the statistical methods as indicated by several reviewers.

Please find our responses below. We hope you agree we've addressed all four of these points.

# Reviewer 1:

The authors present a new Bayesian method to fit movement rates between a set of demes to pairwise genetic differentiation, utilizing a MCMC. They first state the basic equations, which closely resemble existing theory of stepping stone models. They extensively compare their computational method to resistance based methods using an own implementation of the latter, both "under the model" as well as using various quite realistic forward in time simulations. Resistance based methods are much faster and can handle much more demes than the method presented here (no case with more than a 5x5 grid is shown). Therefore, as the authors point out, this work will likely not contest the use of resistance distances for visualizing spatial genetic patterns (which is often done in an exploratory way). But importantly, the method here can infer asymmetric and biased rates, unlike almost all existing methods, which presents a major advance – and certainly fills a niche.

Despite the computational limitations, I believe that this paper will provide researchers a good starting point for future development, by both giving a review about difficulties and also a first idea and example for an implementation.

Overall, I think this article makes a very valid contribution for Molecular Ecology Resources. The authors put their work into the right context and show good knowledge of the relevant literature. The writing is both clear and concise. Importantly, they do not shy away from pointing out the limits of their method, and the very stringent (often unrealistic) assumptions such methods usually make.

I have several comments, but none of them are "make-or-break" or fatal flaws. The manuscript is already in a good state. But I hope the authors can use my comments to further improve their work.

---

**(1.1)** *Clearer point out the current computational limitations of your coalescence time method. It seems it gets tricky with more than about 30 demes? What is the run-time then, does the whole thing blow up? Give an idea how big is too big!*

**Reply**: The runs with 16 demes take around 10 hours with the number of iterations we used (noted in the text, (p. 7, l. 263)). Thirty demes is probably a good limit for the current implementation. There are changes that could be made to make it more efficient for larger systems, but at that point the ill conditioning problem would be more severe because there would be more parameters. We've added a note about this to the discussion. (p. 21, l. 618)

---

**(1.2)** *What is the exact scaling? The bottleneck seems to be calculating the coalescence times with equation (7). You only say that it "can be solved with standard linear algebra". Are you doing Gaussian elimination or something else worse than $N^2$? Do you use any speed-ups to deal with the sparse nature of G for neighbor-only migration? Is it faster than getting the coalescence times by iterating time-discretized recursions? It would be helpful for further progress to describe the exact scaling and the exact algorithm you use.*

**Reply**: In the current implementation, equation (7) is solved using `solve(A,b)` in R. The actual method varies depending on the specific linear algebra library used, but it is typically Gaussian elimination or LU decomposition, both of which are $\mathcal{O}(N^3)$ (unfortunately the decomposition is different in each step; if it were the same it would be $\mathcal{O}(N^2)$). For fine discretizations of space, the matrices are sparse, but in our testing, using sparse matrix methods didn't help at this scale. We've added a point about this last thing to the discussion (p. 21, l. 619) but haven't put in more detail (e.g., plots of scaling with $N$) because it depends on the details (sparsity of the adjacency matrix), and as we discuss above, we think that nonidentifiability is a more serious barrier to finer resolutions.

---

**(1.3)** *The title of the manuscript is a bit misleading. One would not guess that the introduction of a method to infer biased and asymmetric gene flow is the main point. "Isolation by distance" does not appear often in the manuscript, neither its classic literature (Wright, Maryuama, Malecot, Barton etc.) nor direct investigation of genetic differentiation with geographic distance. But these things are also not the scope of this paper.*

**Reply**: We do think a big point of the manuscript is discussion of the drawbacks of resistance-based methods, but we agree with the point about isolation by distance. We've retitled it: "Are populations like a circuit? Comparing isolation by resistance to a new coalescent-based method."

---

**(1.4)** *You could write an outlook stating that your method could be used to fit parameterized models with few parameters. For instance, in case the putative location of a barrier or an area of biased gene flow is known, one could try to infer it without fitting ALL movement parameters, but a simple parametric model, which would implicitly take care of the regularization.*

**Reply**: This is a good thing to emphasize. We've added a bit to this effect. (p. 6, l. 214)

---

**(1.5)** *You use mean absolute error in movement rate to describe the model fit. I believe this measure can be quite misleading for exponential movement rates. Large rates can be notoriously hard to infer (are you super or super-super well connected is almost the same), so it is easy to be off quite a bit, which drives the average absolute error in rate. Also in practice, one does not care so much about absolute rates but "relative" ones. So using a correlation measure $R^{**}2$ of inferred movement rates with actual movement rates would be a very useful and natural fit parameter.*

**Reply**: This is a good point, and we did experiment with other measures of model fit. However, in practice the mean absolute error captured patterns as well as other methods. In the interest of not increasing complexity of the paper, we haven't included results from the other methods.

---

**(1.6)** *You write you use standard methods to check convergence and mixing of the MCMC chain (p. 7, l. 264). Given the degeneracy and the high dimensionality, where there any problems? E.g., local optima you were stuck sometimes? Or was it always pretty straightforward? Maybe write a few sentences on that!*

**Reply**: Convergence could be slow, and the likelihood surface is often ridgy, but we did not see too many problems with getting stuck in completely wrong areas of state space. This the reason we introduced the non-standard "pre-burn-in" phase.

---

**(1.7) (p. 3, l. 91)** $F_{ST} \neq$ *Absolute divergence!!! $F_{ST}$ is more a co-variance measure, and for instance heavily influence by sampling a batch of related individuals (whereas the mean of absolute divergence will be unchanged).*

2

**Reply**: We can't agree more!!!! We've added a note about this, although not a lot of detail, because it seems outside the scope of this paper (p. 3, l. 91). And, we thought we should mention $F_{ST}$ because it is commonly used in these situations.

---

**(1.8)** *You have your own implementation of resistance distance methods, by first extracting hitting times. However, you allow non-symmetric rates, something no existing resistance method would do. Given your observation that there is a lot degeneracy for resistance times (adding skew stuff to hitting times), this introduces uncertainty that likely cannot be broken such as with coalescence methods. This could drive the high uncertainty in Fig. 5 upper right. Given your good results for Fig. 4 for the symmetric case, this is a bit surprising. Maybe run one scheme where you FIX to a single symmetric movement rate between each pair of demes. This setting would be a fairer comparison (and be much closer to what EEMS etc. actually do – they do not even try to infer asymmetric rates).*

**Reply**: We considered doing this, but decided to allow asymmetric migration for resistance distance in order to make the two methods more directly comparable. For instance, how would we compare to the truth if the truth is asymmetric? Comparing methods with both restricted to be symmetric certainly could be useful and informative, but we chose not to include it because it seems not to be the most important comparison (as reality is probably often asymmetric) and we didn't want the paper to get overly complex.

---

**(1.9)** *Maybe describe the model you use for you calculation and inference, a continuous backward in time Markov model with coalescence rates in demes before the actual recursions, and not bit by bit in there.*

**Reply**: We've added a bit more to our big-picture overview that we hope achieves the goal of setting the stage appropriately. (p. 2, l. 82)

---

**(1.10) (p. 5, l. 172)** *Do you actually use this tensor product for the movement rates anywhere? And seems Eq. 7 (which has no tensor product) is all you need.*

**Reply**: We included this because we think it's a nice compact way to write, code, and think about the equation, and the tensor product equation is actually the one used in the R code. It is correct that the equations are equivalent.

---

**(1.11) Line 115:** *Not all ZC skew-symmetric would translate to valid generators $G + Z$. The diagonal elements of G have another condition (they have to be minus the sum of all other jumping rates). Would be interesting to explore this a bit more – overall what the dimensionality this degeneracy is (implicit function theorem), and also if there are simple toy examples where they pop up.*

**Reply**: Thank you for catching this. You are correct that in addition to $ZC$ being skew-symmetric, the rows of $Z$ must also sum to zero, which we now say. (p. 5, l. 178) Further exploration of the constraints would be interesting, but we think is beyond the scope of this paper.

---

**(1.12) Eq. 4:** *H may not be always invertible (H symmetric and positive off-diagonal and 0 on the diagonal is NOT enough). So there might be some pathological cases where multiple G link to one H, maybe even in some simple toy examples.*

**Reply**: Good point; we had not justified this. Under the standing assumption that the chain is irreducible, $H$ is always invertible. We now prove this in the Appendix (p. 29, l. 875), and have made reference to this fact. (p. 4, l. 146)

---

**(1.13)** *Dimensionality arguments ((p. 5, l. 195) and onward) can be a bit misleading when you already know the equations have a non-trivial kernel. Setting all non-neighboring elements of G to 0 might not get rid of parts of the kernel. So maybe flag it even more as "be cautious" as you already have.*

3

**Reply**: Good point; we've changed the wording here. (p. 5, l. 195)

---

**(1.14)** *You could just call the thing by its name: "Stepping stone" model. This term has such a rich history in population genetics!*

**Reply**: In our experience, the term "stepping stone model" is used in a variety of ways in the literature (e.g., also for all-migrate-to-all island models), so we prefer to describe explicitly the grid that we use.

---

**(1.15)** *In the main text, you never mention that the mean of the exponential movement rates for simulations is one, only in a figure. One can also kind of see it from the model figures, but it would be nice to have it explicitly stated in the main text.*

**Reply**: Good point; we've added this. (p. 9, l. 334)

---

**(1.16)** *In the figures, probably keep model figure and inference results closely together. This helps the reader, and makes the figures stand more for themselves.*

**Reply**: This is a good idea, but we haven't been able to see how to implement in a way that would improve things. Maybe we don't see your idea, but the additional graphs that describe population structure in the Appendix won't be legible if added to existing figures, and we think we already have more than enough figures.

---

**(1.17)** *Useful result to know: Maryuama's invariance principle (Nagylaki 1998): That the correctly weighted within coalescence time within demes only depends on the total population size (given conservative migration) – so it cannot fluctuate too wildly across demes and movement rates! This fact motivates why not fitting too wildly differing within-deme coalescence times/diversities.*

**Reply**: Good reference! We'd already referred to the simpler version of Strobeck [1987], and have now added this reference. (p. 30, l. 907)

---

**(1.18) (p. 15, l. 466)** *400,000 generations will look a bit lunatic for someone not in popgen who does not know about rescaling. You could give re-scaled, more realistic values!*

**Reply**: We didn't really intend that number to sound so outlandish, but we think it's more "quite long" than "absurdly long"? We're not sure that mentioning rescaling will help, but have added a reassuring note. (p. 15, l. 466) Note that we *did* actually simulate for that many generations; we didn't use rescaling to run a shorter or smaller simulation.

---

**(1.19) Paragraph beginning (p. 12, l. 404):** *Maybe move this section in front of the inference part, as it is useful to know the most "fundamental" limit of resistance distances.*

**Reply**: This is a good suggestion, but we'd rather keep the different results having to do with the same model together in the same place.

---

**(1.20) Fig. 7:** *With EEMS one can see very suspiciously the 4x4 sampling structure - there are red dots in almost all 3x3 centers of the sampling squares. Since EEMS is quite fast, could you increase the resolution of sampling?*

**Reply**: More samples could be added for the EEMS runs, but doing so would have the drawback that the two methods would no longer be using the same data for inference. We've been told that similar patterns show up when EEMS tries to approximate anisotropic migration, so it may not be the sampling pattern. We've added a note about this. (p. 15, l. 477) Also, note that these samples are more spread out that people

often have in practice: they do occur in the middle three-quarters of each grid square, but they aren't all located at the center.

---

**(1.21)** *You could experiment with visualizations a bit. EEMS got quite popular as exploratory visualization tool because it produces visually pleasing plots. Do lines with two arrowheads of different sizes near the middle, maybe even colored (blue to red) work?*

**Reply**: True! We've tweaked the way the arrows are displayed, and think they look better now.

# Reviewer 2:

> This work revisits McRae's seminal isolation-by-resistance (IBR) model through the lens of co-alescent theory. The original idea of IBR was to compare patterns of genetic distance observed on a landscape with the so-called "resistance distance". The resistance distance between states $i$ and $j$ in a Markov chain is defined to be the "commute time": the expected amount of time it takes for the chain to go from $i$ to $j$ and back, integrated over all possible paths of the chain. Resistance distance comes from electrical circuit theory and is not a model of genetic variation across a landscape. Also, it is inherently symmetric in $i$ and $j$, and cannot accommodate asymmetric migration between demes. A more biologically realistic model is the structured coalescent. Hence, if data are generated under the something resembling the coalescent, then there is scope for improving IBR by reducing model misspecification.
>
> This paper implements such a method and conducts comparative analyses on a number of simulated data sets. It seems that in general, this method and the resistance-based approaches (as exemplified by EEMS) produce somewhat comparable results so long as migration rates are symmetric. The largest differences emerge when gene flow is asymmetric, because this fundamentally violates the resistance distance model used by EEMS. Here, the authors show convincingly that inferring migration rates using the resistance distance approximation can be wildly inaccurate compared to the same estimates obtained using coalescent methods. To the extent that gene flow is more likely to be asymmetric in many natural populations, this seems like an important finding.
>
> My overall impression of this work is fairly positive. The paper is very clearly written, and the idea of replacing IBR with a method that is more faithful to the underlying biology is appealing. The methods section (as well as appendices) feature a very nice and readable summary of the mathematical innovations of this work, as well as some interesting discussion of issues of identifiability and power. Similarly, discussion section in very well done and really strengthens the manuscript. It includes a thorough survey of the related work, as well as a forthright discussion of advantages and disadvantages of the proposed method, and it raises a number of interesting questions and directions for future research. Overall, the paper was a pleasure to read.

Thanks very much for the kind words. One minor comment: resistance distances are not strictly based in a population genetics model, but we think that in practice it is thought of as (an approximation to) such a model – for instance, it is common to see the explanation that it "integrates over all possible paths that the organisms might take". We think McRae [2006] saw resistance distance as an approximation to the more-accurate coalescence models; we're looking at the effects of this approximation. We hope this point comes through in the paper.

> I find the main deficiency to be the lack of any analysis of real data. All experiments are carried out on simulated data only. This is a puzzling omission. The authors went to the trouble of creating an R package (which is good), so clearly they intend for the method to be used in practice. Personally, I would hesitate to publish the results obtained from a method which had not previously been verified to produce reasonable answers in real data. This really

feels like something the authors ought to have included. It is not necessary that the data be novel – reanalyzing (say) the African elephant dataset in the EEMS paper would provide for an interesting comparison (even if it cannot be done at an equivalent spatial resolution) and would also go long way towards reassuring practitioners.

We've now added analysis of a real dataset, from Moreno Geraldes et al. [2014b], and are quite pleased with the results! This has also given us a chance to spend more time talking through how to interpret the results.

---

**(2.1)** *"Bayesian inference of movement rates": In their model the authors assume that many entries of the migration rate matrix are zero, and place an exponential prior on the rest. Is it safe to assume that we will always want to constrain rates between discontiguous cells to zero? Also, given the valid concerns that they raise elsewhere about identifiability and power, I wonder if the authors considered placing a sparse prior on the entire G matrix, enabling the model to adapt to the amount of signal while shrinking other migration rates to zero. This might have the effect of making the resulting non-zero estimates more stable. (I realize that this raises potential problems for inference if the underlying graph becomes disconnected.)*

**Reply**: Whether or not it is reasonable to assume there is no long distance migration depends on the population under study. Putting a sparse prior on all of $G$ is a good idea for future improvement. (Since disconnecting the graph would result in some infinite coalescence times, such proposals would be rejected by the MCMC algorithm.)

---

**(2.2)** *The discussion of ill-conditioning is welcome. From experience, it often feels like coalescent-based methods have little power to accurately estimate migration unless the rates are large. It might be interesting to shift emphasis from estimation to the slightly easier problem of testing: how good are these methods at distinguishing between a given null and an alternative hypothesis (say, barrier vs. no barrier) for the rate matrix G? I think the gain of using a coalescent model might be more apparent in this case.*

**Reply**: This is a good point; we've added it to the discussion (and credited you with it). (p. 21, l. 615)

---

**(2.3)** *This method is computationally limited by equation (7), which has a complexity of $O(d^6)$ for the product Markov chain on d demes mentioned a few lines below. At least, that is the cost for solving (7) exactly – but given the noisiness of the matrix C, there may be little point in doing that anyways. I wonder if the authors have thought at all about obtaining an approximate solution to (7), where the error in approximation is chosen to in some way to balance out the statistical error inherent in C / D. It may also be possible to leverage the fact that the solution G is sparse here. (This is more of a suggestion for future research rather than a suggestion for revision.)*

**Reply**: Thanks for the suggestions. Solving (7) directly for $G$ and $\gamma$ with a noisy $C$ is extremely difficult even in cases small enough to just use least squares; it typically resulted in some negative values unless there is very little noise in $C$. In order to solve for $C$ from $G$ and $\gamma$, we experimented with the Jacobi method. While it seemed to converge fairly reliably, at the grid sizes where it was computationally advantageous to use it over solving exactly, it would still take a very long time for the MCMC to converge due to the large number of parameters. Something along these lines might be useful for finer geographical resolutions, though.

---

**(2.4) (p. 15, l. 456)** *Do the authors have any other guidance on how to discretize the landscape?*

**Reply**: This is a large, thorny issue, closely related to the question of how to translate discrete-population models to continuous geography. We've added a bit more (p. 15, l. 456), as well as some more discussion of this in the section on poplar data. (p. 18, l. 510)

---

**(2.5)** *Does the issue of having negative entries of G (lines 112-117, Appendix A) arise during the course of MCMC sampling, and if so, how is it dealt with?*

**Reply**: No. The proposal distribution includes taking the absolute value of parameters (a standard method in MCMC to preserve reversibility). We've added this note to the MCMC methods section. (p. 7, l. 258)

---

**(2.6) (p. 6, l. 219)** *suggest "commonly" in place of "not uncommonly"*

**Reply**: Changed.

---

**(2.7) (p. 12, l. 406)** *strongly misleading?*

**Reply**: We've reworded this. (p. 12, l. 406)

# Reviewer 3:

> This is an interesting paper on a topic that should be of wide interest to readers of MER. The main results are useful:
>
> 1. landscape genetics models based on resistance theory can be misleading if gene flow is asymmetrical
> 2. coalescent-based models deal better with asymmetry but are not a panacea for a variety of reasons.
>
> On the other hand, I found myself with quite a few questions after reading the manuscript. Raising new questions is not bad in and of itself, but most of these were questions that could/should have been clarified in the text. As a consequence, the manuscript is not as effective or useful as it might be. The problem is not in the writing itself, which generally is careful and precise. Instead, the main problem involves translating a very technical exercise into something that is accessible to typical readers of the journal. Some examples are described below.
>
> Although the theme of the paper is relevant to the journal, I think most readers of MER would find the manuscript hard going in many places. For example, the text at 102-109 and 136-146 would benefit from translation into insights more meaningful to biologists. The authors do a good job of this in discussing results for asymmetric gene flow at lines 296-299.

Thanks for the encouragement. We've tried to improve accessibility in a number of places, in particular by adding a "flag" at the top of the methods (p. 2, l. 85), and improving the two bits of text referred to, at (p. 4, l. 153) and (p. 6, l. 200).

> The reader also needs to understand the biological consequences of various assumptions. Examples where this could be improved include:

---

**(3.1) (p. 3, l. 101)** *if the genome is selectively neutral ...*

**Reply**: Reworded. (p. 3, l. 101)

---

**(3.2) (p. 5, l. 198)** *as long as long distance migration is disallowed*

**Reply**: Added parenthetical clarification. (p. 5, l. 198)

---

**(3.3) (p. 6, l. 231)** *C is large compared to $\sigma$*

**Reply**: Reworded. (p. 6, l. 231)

---

**(3.4) (p. 9, l. 337)**  *we can estimate amount of noise well*

**Reply**: Added explanatory note about how to estimate noise. (p. 9, l. 337)

---

**(3.5)**  *The text at 468ff relating to the assumption of constant pop size and migration rates does a good job of explaining these consequences. Perhaps all assumptions could be listed in a single place and their biological consequences explained.*

**Reply**: The job of enumerating *all* assumptions involved in modeling a real population with a system of discrete demes is daunting. We've put in more discussion of these pitfalls (as described above), but a comprehensive review is beyond the scope of this paper.

---

**(3.6) (p. 3, l. 88)**  *How exactly is the pairwise genetic distance calculated? What does "density of sites" mean? Is it just the fraction of sites at which two genomes differ? If so it is just pairwise theta as used by Wakeley and others.*

**Reply**: That's correct; we've reworded this to be more clear. (p. 3, l. 88)

---

**(3.7)**  *Eq (1): what is $R_{ij}$ and how is q calculated?*

**Reply**: We've added a clarifying sentence. (p. 3, l. 115)

---

**(3.8)**  *G, the movement rate, is clearly a key parameter but is not clearly defined (or if it was I missed it). What are the units of G? Geographic distance per unit time? What are the time units? Years? Generations? If the latter, then does G represent parent-offspring dispersal distance as defined by Wright? Are generations assumed to be discrete? If not, can a migrant leave offspring at various different geographic points?*

**Reply**: A precise definition (in words and equations) is given where it is first introduced, at (p. 3, l. 125). We've rewritten it to be hopefully more clear.

---

**(3.9)**  *As described, the model deals with groups of individuals (populations) that sometimes exchange individuals. But much of landscape genetics/genomics deals with continuously-distributed species that don't have recognizable populations. Are the results also applicable to scenarios like this? Why or why not?*

**Reply**: This is an important point that applies not just to our method but to most methods of population genetics inference, and we view this disconnect as a major unsolved problem in the field. Our simulations of continuous space are explicitly designed to look at this problem. We've added substantially more discussion of this point in the interpretation of poplar results (p. 18, l. 501).

---

**(3.10)**  *The authors identify two sources of noise: Sampling noise (arising from sampling of individuals) and Process noise (stochasticity of population history). Using SLiM, which I gather controls for random variation in the realized pedigree and hence eliminates (or only reduces?) Process noise, the authors obtain estimates for the relative magnitude of the two sources of noise. This is useful but seems incomplete for two reasons:*

1. *A third source of noise is sampling a finite number of genes or SNPs. To some extent one can trade off sampling individuals vs loci, but there are limits to how effective that is.*

2. *The relative magnitudes of the three sources of error are not constant and can vary dramatically depending on parameter values. Process error is inversely related to $N_e$ but otherwise fixed in magnitude; it does not change when sampling errors change. This means that Process error becomes relatively more important when there is a lot of replication in sampling. In particular, genetic sampling error gets very small as the number of SNPs becomes arbitrarily large, in which case it is dwarfed by Process error (e.g., see Figure 6 in our 2009 Mol Ecol paper cited by the authors).*

**Reply**: We certainly had omitted that source of noise, but have added it to the list now (p. 12, l. 432). We agree it can be substantial, but aren't focusing on it here, as the contribution of sampling noise is much less appreciated, particularly in the context of continuous space (see our additional note on this). We're not sure what you mean about SLiM reducing process noise: on the contrary, since we use SLiM to simulate in continuous space, we expect process noise to be larger than in a randomly mating population.

---

**(3.11)** *Also in relation to genomics-scale datasets, two general potential advantages can be identified:*

1. *Arbitrarily large numbers of loci can increase precision and statistical power for existing analyses;*

2. *Ability to access information related to genome structure and function can provide novel insights and make possible qualitatively new types of analyses*

*Lots of people have genomics-scale datasets these days so some discussion of this issue seems important.*

**Reply**: Good point, but to keep the paper relatively focused we're not going into this in detail (but perhaps the pointer at (p. 12, l. 430) suffices?).

---

**(3.12)** *"Can our method replace resistance-based methods? Perhaps, but the substantial uncertainty we saw on graphs with only tens of nodes is indicative of a larger problem we face for realistic models. We have seen that discretization of space results in substantial modeling error, in part because of randomness of geographic sampling and unmodeled process noise can lead to overfitting. Partitioning space into a finer grid should help with these problems, but tends to make the inference problem itself more ill-conditioned: with more connections, changing the value of one connection affects coalescence time less, and so inferences about that value must necessarily be less certain. This tradeoff implies some degree of unavoidable uncertainty. Reproducible, reliable inference will likely require development of new inference methods that explicitly model continuous geography." This seems like a fairly crucial paragraph. But what exactly is the take-home message for biologists interested in practical application of the methodology?*

**Reply**: Good question! As written, the take-home was "wait until we make better methods", but we've added a better one. (p. 18, l. 535)

---

**(3.13)** *Coalescent rates are critical to model performance, which can be poor if the rate is too low. It is obvious that the coalescent rate is inversely related to $N_e$, but in practical terms, what does it mean when the coalescent rate is lowered from 10 to 0.1?*

**Reply**: We've added more context to this section. (p. 9, l. 365)

---

**(3.14) (p. 9, l. 348)** *"we varied the standard deviation of the noise from 1/1000th to 1/50th of the mean value of C for that grid." This sounds like a CV of 0.001 to 0.02 for noise, both of which would be exceedingly small. If that is not what is meant, please clarify. (p. 9, l. 348)*

**Reply**: That is what we mean, and although small, we don't think that's unreasonable for genome-scale data under a discrete population model (but see our later discussion of process noise). We realize that many people are working with much smaller number of (ascertained) loci, but there's enough bigger issues here related to continuous geography that we've not explored in that direction.

---

**(3.15) (p. 22, l. 635)** *"if fecundity is variable" – on what scale? Among populations? Among individuals? Among ages within the same individual?*

**Reply**: We mean among individuals (and have added this). (p. 22, l. 635)

---

**(3.16) (p. 7, l. 254)** *"It is not required in this approach to have samples from every spatial location ..."* *Required for what? Are they saying that unsampled but real (ghost) populations have no effect on precision or bias?*

**Reply**: We're saying that it is possible to *run* the method to have samples in each location – so it is easy, in principle, to include "ghost" populations. Of course, unsampled populations will affect accuracy of the result, and we've added a note to clarify. (p. 7, l. 254)

---

**(3.17)** *Many of the figures are too small to read easily without a magnifying glass. Figures 3-5 are large enough but they include miniscule fonts that make it impossible to tell exactly what is plotted. Green and black do not provide enough contrast.*

**Reply**: We sympathize, and have increased the sizes of most of the labels. However, the x-axis labels of figures like Figure 3 cannot be made larger without overlapping, and we'd like to keep them. Another approach would be to simply plot true versus observed values, which is equivalent to the current plot without the x-axis labels. We prefer to leave these labels, even if these are only really legible in the digital version (after zooming in).

---

**(3.18) (p. 1, l. 24)** *another limitation of direct observations is that they only provide information about movement of individuals but not gene flow, which requires successful breeding*

**Reply**: Good point, but we'd like to keep this bit more concise.

---

**(3.19) (p. 2, l. 62)** *the "wrong answer" compared to what?*

**Reply**: The truth. We've changed the phrasing. (p. 2, l. 62)

---

**(3.20) (p. 2, l. 67)** *What is EEMS?*

**Reply**: A lengthy acronym (that we've added, as well as MAPS, later). (p. 2, l. 67)

---

**(3.21) (p. 2, l. 71)** *What exactly is a more general problem?*

**Reply**: Clarified. (p. 2, l. 71)

---

**(3.22) (p. 3, l. 89)** *need a semicolon, not a comma, after "two genomes"*

**Reply**: We reworded this.

---

**(3.23) (p. 7, l. 267)** *why quotes for "from the model"?*

**Reply**: Removed. (p. 7, l. 267)

---

**(3.24)** *"suppose that the spatial arrangement of populations is given by a graph ..." "Graph" is a very general term and not clear exactly what is meant here. If the word has a more specific meaning in this context, please define it.*

**Reply**: Done. (p. 6, l. 242)

---

**(3.25) Fig 6 caption:** *the barrier is "sufficiently thick" to prohibit migration. "Thick" implies distance, but is that a requirement? Couldn't the barrier be higher or deeper or less penetrable for a different reason than thickness?*

**Reply**: It could, but this is the way we implemented it in the simulation.

# Reviewer 4:

This is a polished theoretical and methodological contribution towards understanding the genetic processes that affect genetic distance and thus connectivity of species across the landscape. The authors make a little-appreciated point about considering the coalescent time as a predictor of genetic distance as opposed to resistance distance which can result in spurious results where genetic distance is shaped by asymmetrical gene flow and coalescent processes.

There are some points of clarification however that I think need to be made so that the paper is accessible and clear to its intended audience, and to ensure the paper can be adopted and influence analyses in this area. The differences in the highly spatial resistance distance approach versus the genetics-based coalescent time-based approach need to be distinguished more clearly, as in some ways this may be seen as comparing apples and oranges. Issues around timescales of genetic change (effects of landscape vs coalescent times) need to be further addressed and elucidated. The differences in the results gained from the approaches are clearly defined and presented however.

The types of questions and the type of demographic scenarios under which resistance vs. coalescense based approaches may be an improvement, or combined in the same study should be made more clearly. I suggest a summarising table or flow chart to this effect, that addresses time scales also.

We've added more discussion along these lines particularly in (p. 21, l. 620) and in relation to analysis of the poplar data. We've got quite a few figures already (and have added one for the poplars), so haven't tried to add a flow chart.

---

**(4.1) Line 7 of abstract and generally:** *This statement is conditional on the characteristics of the data you have, and your study aim. If the study aim is to ask how landscape features affect genetic distance, then the coalescent time is not going to explicitly test this, or? It needs to be made clear how different study objectives will benefit in landscape genetics and under what circumstances a 'more accurate' predictor of genetic distance can be gained. It seems appropriate to mention that this approach would greatly complement existing landscape genetic analysis approaches to see the relative effects of resistance and coalescent time. Implications for management decisions based on resistance models could be mentioned, as resistance models are intended to inform conservation decisions in some cases.*

**Reply**: We're not sure which possible study aims are being referred to, but one possible aim that is not possible currently with coalescence methods is to produce high-resolution maps (as we discuss, (p. 20, l. 543)). We made the statement that genetic data are more accurately modeled by coalescence time than resistance distance because while there is an extensive literature describing the broad conditions under which coalescence is a good model for the process that produces genomic data, we know of no such justification for resistance distance. Perhaps the key disconnect here is that we're thinking about generative models? We agree that since coalescence theory does not always apply, resistance distance on some network could in principle be closer to the truth than any coalescence times. However, we're unaware of this claim having been made. Furthermore, as we understand it, the point of landscape genetics methods using resistance distance is not merely to recapitulate observed genetic distances, but to provide an accurate depiction of past or present gene flow, i.e., movements of individuals across the landscape, In our paper we've tried to describe how inaccuracies of the generative model that underlies resistance distance can lead to misleading results. The only downside to coalescence time inference is computational tractability (discussed at (p. 18, l. 521)): otherwise, one can be swapped out for the other. In fact, *any* method that uses resistance distances could in principle be done with coalescence times instead (e.g., to look at the effect of landscape features). This is discussed at (p. 21, l. 589).

---

**(4.2) (p. 1, l. 33)** *Extremely long sentence, please divide.*

**Reply**: Done. (p. 1, l. 33)

---

**(4.3) (p. 9, l. 362)** *Would it make sense to select genetic markers that are more informative for coalescence rates by narrowing the level of variation accepted in the model? Would this help error rates justifiably or just bias interpretation?*

**Reply**: This is an interesting idea, and suggests looking at a statistic of genetic differentiation other than the mean, perhaps IBD segment lengths (as done by Al-Asadi et al. [2018]). We don't know enough about this to speculate, however.

---

**(4.4) (p. 12, l. 396)** *I think it might be helpful if this point was made earlier and reiterated*

**Reply**: Done, at (p. 3, l. 119).

# Reviewer 5:

This article focuses on the inference of gene flows between populations from the analysis of georeferenced genetic data. In particular, a new coalescent-based technique, which applies to the analysis of pairs of sampled individuals, is compared to an approach based on "resistance distances" which aim at approximating coalescent distances. This work is interesting because resistance distances are at the core of several popular techniques in landscape genetics. It is thus important to gain a good understanding of how good this phenomenological approximation is compared to more mechanistic techniques such as the structured coalescent. The article clarifies the connections between the two approaches in a convincing manner. It thereby fully deserves to be published in Molecular Ecology Resources. There are however a few points (see below) that I think should be improved should the authors see fit.

---

**(5.1)** $Pr(X_{t+e} = y|X_t = y)$ *should read* $Pr(X_{t+e} = y|X_t = x)$.

**Reply**: Whoops, thanks! (p. 3, l. 127)

---

**(5.2)** *Regarding Equation 2, I would recommend giving more detail explaining where this comes from. Here is a suggestion:*

$$H_{xz} = dt + \sum_y Pr(X_{dt} = y|X_0 = x)H_{yz}$$
$$= dt + \sum_{y!=x} Q_{xy}dtH_{yz} + (Q_{xx}dt + 1)H_{xz}$$

**Reply**: We wondered whether this would overload readers, but have now included an explanation along these lines. (p. 4, l. 135)

---

**(5.3)** *On a related note, it might be helpful to give more explanations about Equation 6. In fact, I am not quite sure I agree with it. Indeed, for $x \neq z$, we have*

$$C_{xz} = dt +$$
$$1/2 \sum_y Pr(X_{dt} = y | X_0 = x) C_{yz} +$$
$$1/2 \sum_y Pr(X_{dt} = y | X_0 = z) C_{xy},$$
$$= dt +$$
$$1/2 \sum_{y \neq x} Q_{xy} dt C_{yz} + (Q_{xx} dt + 1) C_{xz} +$$
$$1/2 \sum_{y \neq x} Q_{zy} dt C_{xy} + (Q_{xx} dt + 1) C_{xz},$$

*where the 1/2 terms correspond to the probability of "selecting" the lineage found in x (resp. z) at time 0 to move to y after dt. The last equation above then gives*

$$-2 = \sum_y Q_{xy} C_{yz} + Q_{zy} C_{xy}$$

*which differs from the one given in the ms. I have probably missed something in the derivation used by the authors. Giving a few more explanations here might help avoiding any confusion.*

**Reply**: Besides substituting $G$ for $Q$, our equations only differ by the factor of $1/2$. The model we work under is that each lineage moves as an independent copy of the Markov chain $X$, so that the total jump rate when the two chains are at $x$ and $z$ is $-G_{xx} - G_{zz}$. We think the factors of $1/2$ are in error – a more clear way to see this would be to say that $X$ and $Z$ are the locations of the two lineages, that move independently according to $G$ until they coalesce, and so

$$C_{xz} = dt +$$
$$\sum_u \mathbb{P}(X_{dt} = u | X_0 = x) C_{uz} +$$
$$\sum_v \mathbb{P}(Z_{dt} = v | Z_0 = z) C_{xv},$$
$$= dt +$$
$$\sum_{u \neq x} G_{xu} dt C_{uz} + (G_{xx} dt + 1) C_{xz} +$$
$$\sum_{v \neq x} G_{zv} dt C_{xv} + (G_{xx} dt + 1) C_{xz}.$$

---

**(5.4)** *I was also a bit puzzled by the likelihood function that is at the core of the Bayesian inference proposed here (see Equation 8). The spatial component of the data seems completely hidden. It is in fact conveyed by the coalescent times $\mathcal{C}_{ij}(G, \gamma)$ but a more detailed description of the likelihood function where both genetic and spatial information appear explicitly would facilitate the understanding of the proposed inference technique.*

**Reply**: We've added a clarifying sentence. (p. 7, l. 248)

---

13

**(5.5)** *Moreover, my understanding is that the joint probability of the pairwise genetic distances ($D$) and spatial locations ($L$) given $G$ and $\gamma$, i.e., $p(D, L|G, \gamma)$, is expressed as the product $p(D|L, G, \gamma) \times p(L|G, \gamma)$. Thanks to Equation (7) the first density is in fact $p(D|C)$, where $C$ are the coalescent times. The authors use a normal distribution for $D|C$ but nothing is said about the distribution of $L|G, \gamma$. It is paramount to explicitly define every probabilistic distribution in the likelihood of the model used for the inference so as to clarify what are the underlying simplifying hypotheses the proposed approach relies on.*

**Reply**: In our model, spatial locations are (discrete and) assumed to be known without error, and we do not want to model the sampling process, so they do not enter into the likelihood. Also recall that both $D$ and $C$ are *complete* matrices of genetic distances and pairwise coalescence times – i.e., between all pairs of populations – so the locations do not enter at this stage (although they are certainly used in estimating $D$). We have added a note reminding the reader of this. (p. 7, l. 246)

---

**(5.6)** *On a related note, my understanding is that the uncertainty affecting coalescent times conditional on the movement rates is not taken into account in the proposed approach (i.e., knowing $G$, one gets $C$ through Equation 7 in a deterministic fashion). I would recommend that the authors discuss this point.*

**Reply**: This is true; we've added a sentence emphasizing this. (p. 6, l. 234)

---

**(5.7)** *The sentence "with noise standard deviation equal to 1/1000th of the mean coalescence time (left) and 1/100th of the mean coalescence time (right)" should read "with noise standard deviation equal to 1/1000th of the mean coalescence time (top) and 1/100th of the mean coalescence time (bottom)"*

**Reply**: Whoops! Fixed. (p. 10, l. 378)

---

**(5.8)** *The authors call for new models to be developed that would properly accommodate for individuals distributed in space along a continuum as opposed to discrete demes, as is the case with the structured coalescent. The spatial Lambda-Fleming Viot model is one of these. It has been studied extensively from a mathematical standpoint (see the body of work by Etheridge, Barton and Veber amongst others) and has been used for the inference using a Bayesian approach (see Guindon, Guo, Welch, Theoretical Population Biology, 2016; but also Koskela's PhD thesis `http://wrap.warwick.ac.uk/88065/1/WRAP_Theses_Koskela_2016.pdf`). The spatial Lambda-Fleming-Viot model is mechanistic and enjoys many good statistical and biological properties (e.g., it does not suffer from the "clumping" issue that affects the Wright-Malecot model).*

**Reply**: Certainly! We agree that the SLFV model is a promising way forward to be able to use coalescent simulations in continuous space. There's a lot of work left to explore how and when it's a good approximation to reality also, but we've added a bit about it to the "Other methods" section. (p. 20, l. 567)

---

**(5.9)** *Assuming that space is discrete in arguably the biggest weakness of the structured coalescent. It is quite often not biologically realistic and breaks down mathematically when considering larger numbers of smaller demes. The spatial Lambda-Fleming-Viot avoids this important shortcoming and thus probably deserves more attention.*

**Reply**: We agree, and very much hope to move in that direction. We've added more discussion of this. (p. 20, l. 571)